

A PETROGENETIC STUDY
OF THE
GUICHON CREEK BATHOLITH, B.C.

by

Christopher J. Westerman
B.Sc. University of London, 1967

A THESIS SUBMITTED IN PARTIAL FULFILMENT OF
THE REQUIREMENTS FOR THE DEGREE OF
MASTER OF SCIENCE

in the Department
of
GEOLOGY

We accept this thesis as conforming to the
required standard

THE UNIVERSITY OF BRITISH COLUMBIA

April, 1970

In presenting this thesis in partial fulfilment of the requirements for an advanced degree at the University of British Columbia, I agree that the Library shall make it freely available for reference and study.

I further agree that permission for extensive copying of this thesis for scholarly purposes may be granted by the Head of my Department or by his representatives. It is understood that copying or publication of this thesis for financial gain shall not be allowed without my written permission.

Department of GEOLOGY.

The University of British Columbia
Vancouver 8, Canada

Date April 23rd. 1970.

ABSTRACT

The Guichon Creek batholith is exposed approximately 200 miles N.E. of Vancouver, B.C. and is a zoned 'granitic' pluton of Lower Jurassic age (198 ± 8 my). The batholith consists of seven major intrusive phases. The predominant rock type is granodiorite with lesser amounts of quartz diorite and quartz monzonite.

Study of rock and mineral compositions has revealed a gradual variation in the relative proportions of mineral phases as crystallisation of the batholith proceeded. The chemical compositions, however, of the individual mineral phases show very little change. The relative roles of assimilation and magma convection in producing compositional variations in the early phases of the batholith are discussed.

Alkali feldspars are microperthitic with bulk compositions in the range 71-86 Wt% Or and the compositions of the perthitic components approach pure end members. The potassic phases of the perthites have structural states equivalent to that of orthoclase. The plagioclase feldspars are oligoclases with low to intermediate structural states. Plagioclase from the early phases of the batholith (Hybrid and Highland Valley phases) show normal zoning whereas those from

the later phases (Bethlehem and Bethsaida) show oscillatory zoning. Biotites from the major phases of the batholith have progressively lower $\text{Fe}/(\text{Fe}+\text{Mg})$ ratios with progressively increasing silica content of the host rocks. Plagioclase crystallized early in the older phases of the batholith whereas quartz was the early mineral to crystallize from the younger major phases.

Evidence suggests that magma convected during crystallisation of the older phases of the batholith but that the younger phases crystallised from a stationary magma. Comparisons with experimental systems suggest that the early magma crystallised under conditions of relatively low total pressures in the order of 1 or 2 kb but that the later phases may have been subjected to total pressures in the order of 4 or 5 kb during crystallisation. This increase in total pressures was most probably due to increasing volatile pressures during crystallisation.

LIST OF CONTENTS

	<u>PAGE</u>
I Introduction	1
II Geologic setting of the batholith	5
III The Alkali feldspars	
a. Mode of occurrence	9
b. Method of study	9
c. Compositions of the Natural Alkali Feldspars	15
d. Structural states of the Natural Alkali Feldspars	17
e. Bulk compositions of the homogenised alkali feldspars	25
IV The Plagioclase Feldspars	
a. Mode of occurrence	27
b. Plagioclase Compositions and Zoning	27
V The Biotites	
a. Mode of Occurrence	42
b. Method of Study	44
c. Discussion of Results	46
VI Modal Analyses and Calculated Chemical Compositions	56
VII Geological evolution of the batholith	72
VIII Summary and Conclusions	83

	<u>PAGE</u>
References Cited	90
Appendix 1. Petrographic descriptions	95
2. Modal analyses and calculated chemical compositions	102
3. Biotite electron microprobe analysis - experimental procedures	110

LIST OF TABLES

TABLE	PAGE
I. Phases and varieties of intrusive rock	4
II. Unit cell parameters of K rich phases in alkali feldspars	11
III. Compositions of the perthitic phases of the alkali feldspars, and data plotted in Fig.5 .	13
IV. Unit cell parameters for homogenised alkali feldspars	14
V. Relation between estimated bulk composition and degree of anomaly for computer refined alkali feldspars	19
VI. $^{\circ}2\theta$ values for $\bar{2}01$ reflections ($\text{CuK}\alpha$) and estimated bulk compositions of homogenised alkali feldspars from the Guichon Creek batholith	26
VII. Table of plagioclase compositions	28
VIII. Observed X-ray intensity ratio $I_{\frac{004}{005}}$ for 3 biotite samples as a function of sample preparation	45
IX. Results of partial electron-microprobe analysis of biotites from the Guichon Creek batholith	48
X. Criteria, suggested by Buddington (1959) as indicative of mesozonal intrusion which are present in the Guichon Creek batholith	80
XI. Electron microprobe analyses of biotite standards. Data used in construction of Fig. 17	115

LIST OF FIGURES

FIGURE	PAGE
1. Geology of the Guichon Creek batholith	3
2. Sample location map	8
3. Orthoclase content of alkali feldspars plotted as a function of the <u>a</u> cell dimension, unit cell volume and $^{02\theta}$ $\overline{201}$ $\text{CuK}\alpha$. Simplified from Wright and Stewart (1968) and Wright (1968)	16
4. Refined cell parameters for alkali feldspars from the Guichon Creek batholith plotted on a <u>b</u> - <u>c</u> plot, simplified from Wright and Stewart (1968)	18
5. Alkali feldspars from the Guichon Creek batholith plotted on a $060 - \overline{204}$ ($^{02\theta}$ $\text{CuK}\alpha$) plot, simplified from Wright (1968)	18
6. X-ray diffraction pattern for sample 31 in the region of $30^{02\theta}$ $\text{CuK}\alpha$	22
7. Modal feldspar constituents of the Guichon Creek batholith samples recalculated to 100% An+Ab+Or	33
8. Plagioclase zoning schemes	36
9. Compositions of plagioclases in equilibrium with granitic melts as a function of temperature at 2kb water pressure (From Piwinski, 1968, p. 560)	40
10. Relation between abundance of biotite and silica content of host rock	43
11. Biotite compositions as a function of the silica content of the host rock	47
12. Stability of biotites as a function of $f\text{O}_2$ and temperature at 2070 bars total pressure (From Wones and Eugster, 1965)	50

<u>FIGURE</u>		<u>PAGE</u>
13a.	Plot of modal quartz-orthoclase-albite-anorthite for the Guichon Creek batholith samples	55
b.	Schematic phase diagram for the ternary system Qz-Or-Ab-An at 1 kilobar water vapour pressure	55
14.	Calculated component oxides plotted as a function of silica content for the Guichon Creek batholith samples	64,65
15.	Chemical compositions of proposed Guichon Creek batholith primary magma, 'contaminated' Guichon rocks and Nicola Group extrusive rocks	68
16.	Summary of compositional variations in the Guichon Creek batholith	82
17.	Microprobe analyses. Total counts observed as a function of composition for biotite standards	114

LIST OF PLATES

PLATE	PAGE
1. Partially resorbed plagioclase enclosed within poikilitic alkali feldspar. Sample #11. Chataway variety. Crossed nicols, x 30	31
2. Partially resorbed plagioclase enclosed within poikilitic alkali feldspar. Sample #10. Chataway variety. Crossed nicols, x 30	31
3. Partially resorbed, oscillatory zoned plagioclase enclosed in poikilitic, perthitic alkali feldspar. Note the albitic rim to the plagioclase. Sample #25, Bethlehem phase. Crossed nicols, x 30.	35
4. Oscillatory zoning in plagioclase. Sample # 34, Bethsaida phase. Crossed nicols, x 30	35
5. Sample from a chilled Bethsaida dyke from east of the Bethlehem Copper property. Note presence of subhedral-euhedral phenocrysts of quartz and euhedral poikilitic biotite. Scale in centimetres..	62

ACKNOWLEDGEMENTS

The author wishes to express his thanks to Drs. K.C. McTaggart, E.P. Meagher and J.A. Gower who acted as thesis supervisors. Thanks are also due to Dr. K.E. Northcote of the British Columbia Department of Mines and Petroleum Resources who supplied all the samples used, to Dr. J.H.Y. Rimsaite of the Geological Survey of Canada who supplied chemically analysed biotites and to M. Osatenko of Cominco Ltd., Geological Research division who provided chemical analyses of the biotite standards supplied by Dr. J.A. Gower.

I Introduction

The Guichon Creek batholith crops out over an area of approximately 400 sq. miles near to and southeast of the town of Ashcroft in the Interior Plateau of British Columbia. The batholith is of considerable scientific and economic interest. The Bethlehem Copper and Craigmont Mines, and several potential mines such as Lornex and Valley Copper occur within or adjacent to the batholith.

Early geological mapping of the eastern half of the Guichon Creek batholith, at a scale of 4 miles to 1 inch, was completed by W.E. Cockfield (1947), and of the western half by S. Duffell and K.C. McTaggart (1952). Several detailed reports of parts of the batholith have been prepared by J.M. Carr (1959-1963) and the geology of mineral deposits associated with the batholith has been described by W.H. White, R.M. Thompson and K.C. McTaggart (1957). Radiometric K/Ar age determinations from the batholith have been published by Baadsgard et al (1961), Dirom (1965), Wanless et al (1965, 1967), White et al (1967), and Northcote (1968, 1969). Christmas et al (1969) have studied the rubidium/strontium, sulphur and oxygen isotopic composition of samples from the batholith and the

associated Craigmont ore body. Previous work on the batholith culminated in a detailed geologic and geochronologic study by Northcote (1969). Northcote mapped seven separate intrusive phases of the batholith, described them, and explained the differences between them as due to the combined action of assimilation and magmatic differentiation. In addition Northcote proposed that a change from mesozonal to epizonal environments occurred during emplacement of the pluton.

The present work was undertaken as an attempt to further describe the mineralogy of the various phases and the mechanisms involved in the emplacement of the batholith. It was hoped that the differentiation occurring within the pluton would be reflected in the changing compositions of feldspars and biotites which occur throughout the batholith. In addition it was hoped that study of the variation in the structural states of the alkali feldspars would help in determining the history of crystallisation and changes in the environment of emplacement of the batholith.

All of the samples used in the present investigation were collected by Dr. K.E. Northcote during the preparation of his Ph.D thesis (University of British Columbia) in the summers of 1963 and 1964.

FIG. 1: GEOLOGY OF THE GUICHON CREEK
BATHOLITH

Simplified from
Northcote (1969).

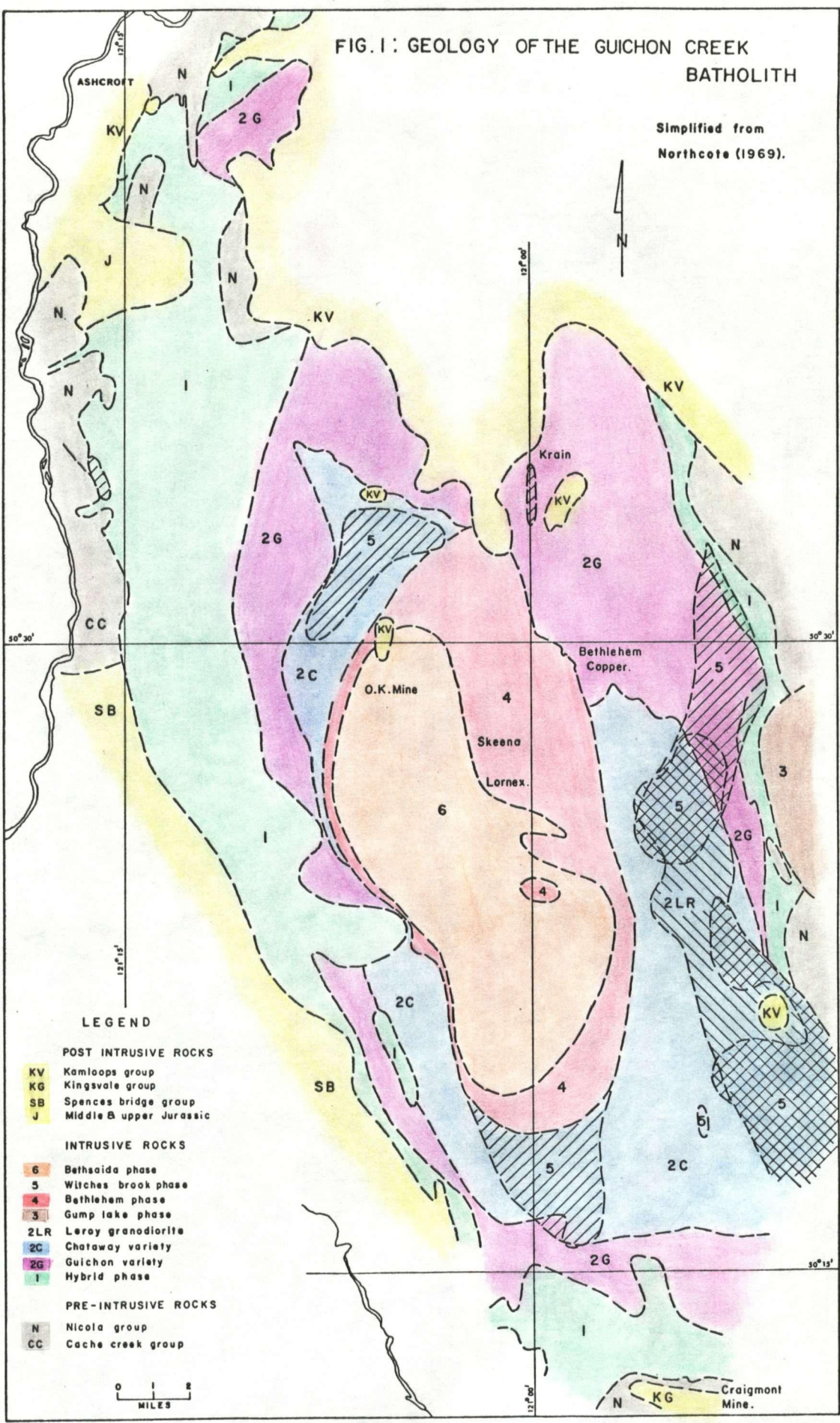


TABLE I
Phases and Varieties of Intrusive Rocks
 (from Northcote 1969)

Relatively Old

- (1) Hybrid phase - quartz diorite, granodiorite
- (2) Highland Valley phase
 - (2G) Guichon variety - quartz diorite, granodiorite
 - (2C) Chataway variety - granodiorite, quartz monzonite
 - (2LR) LeRoy granodiorite - granodiorite, quartz monzonite

Intermediate Age

- (3) Gump Lake phase - granodiorite, quartz monzonite
- (4) Bethlehem phase - granodiorite, quartz monzonite
- (5) Witches Brook phase
 - Variety A - granodiorite
 - Variety B - granodiorite
 - Variety C - granodiorite, quartz monzonite, granite
- Bethlehem porphyries

Relatively Young

- (6) Bethsaida phase - quartz monzonite, granodiorite
- (7) Gnawed Mountain porphyries, younger Bethlehem porphyries and associated intrusive breccias
 - Leucocratic dykes and irregular-shaped bodies

II Geological Setting of the Batholith

The general geology of the Guichon Creek batholith has been described by Northcote (1968, 1969) and only a brief summary will be given here.

The batholith is a semiconcordant, zoned, 'granitic' pluton consisting of several intrusive phases arranged in a roughly concentric pattern. The batholithic rocks intrude sedimentary rocks of the Cache Creek Group (Permian) and Nicola Group (Karnian stage: Upper Triassic) causing local contact metamorphism to albite-epidote or hornblende hornfels facies. The batholith is overlain unconformably by Middle and Upper Jurassic sediments and Lower Cretaceous and Tertiary volcanic and sedimentary rocks. There is no evidence of any significant metamorphic activity occurring in the region after emplacement of the batholith. Published radiometric age determinations of rocks from the batholith give an average age of approximately 198 my. (Dirom, 1965; Wanless et al 1965, 1967; White et al 1967; Northcote 1969; Christmas et al, 1969).

Northcote has divided the batholith into seven major phases (Table I, Fig. 1) primarily on field relationships and textural variations. Most of the batholith is composed of granodiorite, with lesser

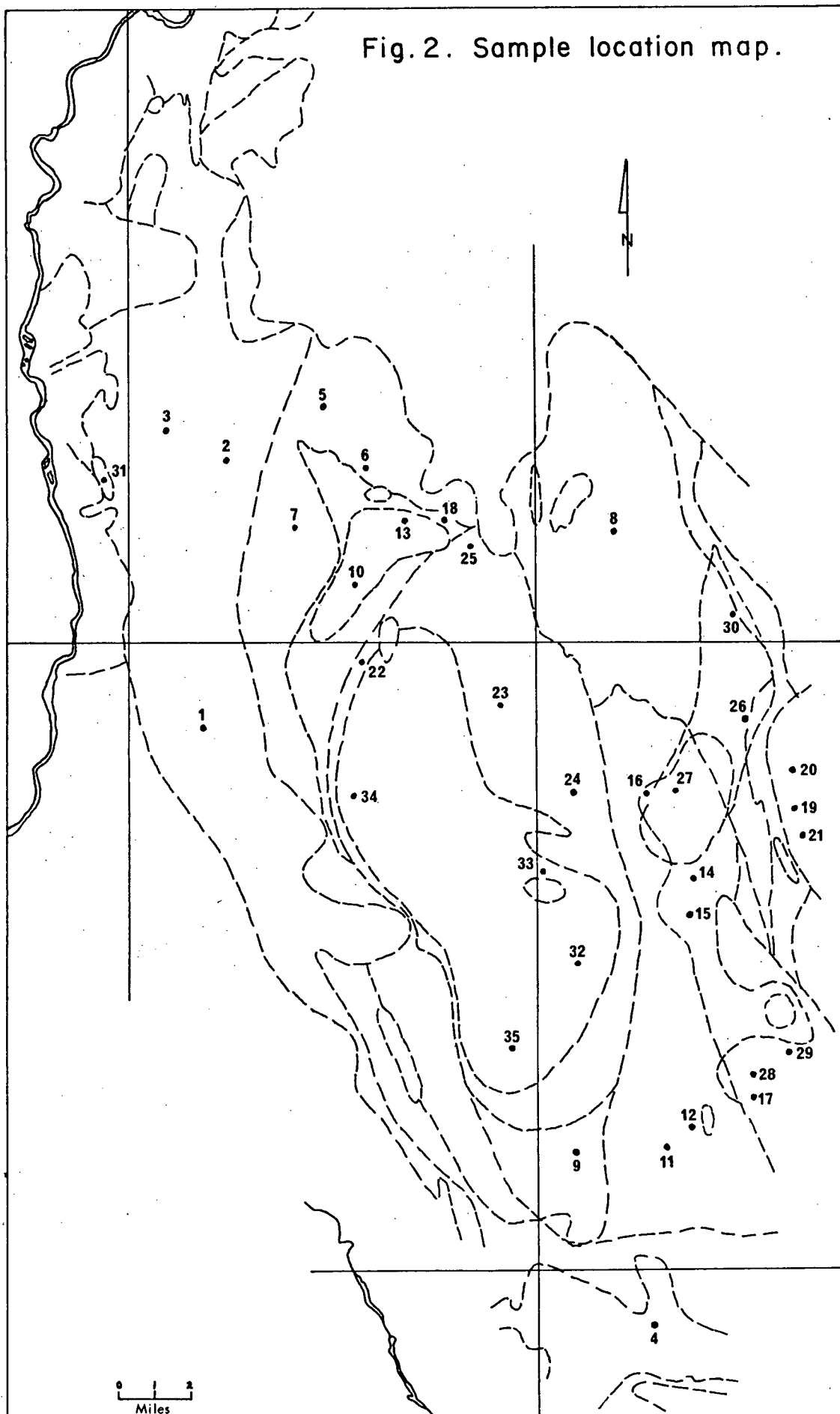
amounts of quartz diorite, quartz monzonite and with minor granite. In a general way the older phases tend to be basic, the younger phases to be acidic. Northcote has suggested that the Guichon variety granodiorite may approximate the composition of the original magma and that the more basic rocks may be the result of contamination, the more acidic rocks the result of differentiation of this magma.

The roughly concentric pattern of the major phases of the batholith is disrupted by three of the minor phases. The Gump Lake phase occurs as a semiperipheral body on the eastern margin of the batholith, the LeRoy and Witches Brook phases occur as irregular dyke-like bodies within older phases. Contacts between phases range from sharply intrusive to broadly gradational and a single contact may vary in nature along its length. Chilled contacts between phases are extremely rare and for this reason Northcote considers that all phases were hot at approximately the same time, inferring only a short time interval between intrusive pulses. The major phases of the batholith have a coarse-grained, hypidiomorphic texture, and only the youngest, minor phases include porphyritic rocks. The Hybrid, Highland Valley, Witches Brook and parts of the Bethlehem phases

all exhibit, to varying degrees, alignment of plagioclase crystals. In addition a rough foliation of mafic minerals is present, locally, within the Guichon variety.

On the basis of textural evidence, Northcote (1969) has suggested that the early phases of the batholith were emplaced under mesozonal conditions and that progressive erosion of the cover rocks established epizonal conditions during emplacement of the later phases.

Fig. 2. Sample location map.



III The Alkali Feldspars

a) Mode of Occurrence

The rocks investigated contain between 1% and 20% alkali feldspar, most of which is either interstitial or poikilitic, enclosing plagioclase, quartz, hornblende and biotite. As a general rule fine-grained rocks contain interstitial alkali feldspar whereas in coarse grained rocks it is poikilitic. All the samples investigated are either microperthite or cryptoperthite in which the subordinate, albite-rich phase occurs as extremely thin stringlets. (c.f. Alling, 1938, p.142). Wherever poikilitic alkali feldspar is in contact with plagioclase the alkali feldspar either forms embayments in the plagioclase, or myrmekitic intergrowths are present within the plagioclase marginal regions. The significance of these features is discussed in chapter IV.

b) Method of Study

Alkali Feldspars were separated from the 80-120 mesh fraction of the crushed and sieved rock using a combination of electromagnetic and heavy-liquid methods. Magnetite and other strongly magnetic minerals were first removed from the size fraction with a hand magnet. The remaining material was then passed through a Franz

electromagnetic separator set at maximum amperage, to remove mafic minerals and any heavily altered feldspar. The remaining fraction was then processed by separation in bromoform diluted with acetone to a specific gravity such that a quartz crystal sank and an orthoclase crystal floated in the mixture. The "float" fraction from this final separation consists of alkali feldspar with very minor amounts of adhering quartz. The "sink" fractions consist mainly of discrete quartz and plagioclase grains with minor but variable amounts of composite grains and occasional non-magnetic mafic minerals.

Smear mounts were made of each sample and three X-ray diffractometer patterns were run for each using CaF_2 ($a = 5.4631 \pm .0006 \text{\AA}$) as an internal standard. The runs were made using Ni filtered Cu radiation from a 2θ angle of 58° to 19° , at a scan speed of $\frac{1}{2}^\circ/\text{min}$. and chart speed of $2\text{cm}/\text{min}$.

For twelve of the samples all peaks present were measured and indexed using the tables given by Wright and Stewart (1968). Unit cell parameters (Table II) for the K-rich phase in these samples have been calculated using the 'variable-indexing' computer program developed by Evans, Appleman and Handwerker (1963) of the U.S.G.S.

TABLE II UNIT CELL PARAMETERS OF K RICH PHASE IN ALKALI FELDSPARS

Sample #	Phase	Wt% Or	a(Å) °	b(Å) °	c(Å) °	α	β	γ	V(Å) ³ °	No. of lines used	Std. error (°2 θ)
3	1	92.0	+8.581 - .003	12.984 .003	7.205 .001	90°	116° 2.55' 1.45'	90°	721.18 .30	18	.017
4	1	92.0	+8.575 - .002	12.994 .002	7.201 .001	90°	116° 1.59' 1.02'	90°	721.06 .18	15	.009
6	2G	91.5	+8.576 - .004	12.985 .003	7.203 .001	90°	116° 2.23' 1.29'	90°	720.79 .31	13	.013
12	2C	91.5	+8.573 - .004	12.987 .003	7.204 .002	90°	116° 1.08' 1.58'	90°	720.90 .36	15	.016
13	2C	92.0	+8.577 - .005	12.988 .004	7.203 .002	90°	116° 2.49' 1.70'	90°	721.02 .42	14	.017
17	2LR	88.5	+8.555 - .007	12.989 .005	7.208 .002	90°	116° 3.29' 2.05'	90°	719.60 .60	13	.023
19	3	92.0	+8.580 - .005	12.985 .004	7.206 .002	90°	116° 3.04' 1.98'	90°	721.13 .45	12	.018
22	4	96.5	+8.584 - .003	12.988 .002	7.206 .001	90°	116° 1.46' 0.97'	90°	721.97 .23	14	.010
23	4	93.0	+8.578 - .003	12.992 .003	7.204 .001	90°	116° 0.16' 1.45'	90°	721.57 .27	17	.016
27	5	90.5	+8.564 - .002	12.990 .002	7.206 .001	90°	116° 0.22' 0.75'	90°	720.46 .16	18	.009
29	5	89.0	+8.562 - .004	12.980 .003	7.208 .002	90°	116° 2.29' 1.77'	90°	719.79 .40	12	.013
33	6	92.5	+8.581 - .003	12.985 .003	7.204 .001	90°	116° 1.35' 1.36'	90°	721.32 .28	14	.014

Input for the calculations was restricted to those reflections that could be uniquely indexed and which showed a total deviation of less than 0.015° 2θ from three diffractometer patterns. Following the precedent of Wright and Stewart (1968) the majority of the peaks have been measured as close as possible to the maximum peak height. However, in uncertain or ambiguous cases, peaks were measured at the $2/3$ peak height position. For the remaining samples the positions of the 060, $\bar{2}04$, and $\bar{2}01$ reflections for the K-rich phase, and the $\bar{2}01$ reflection for the Na-rich phase, have been measured. (Table III). All the samples investigated contain both a K-rich, and an Na-rich phase and hence there is the chance of mutual interference for some of the reflections. In most of the samples, however, the Na-rich phase was greatly subordinate - as estimated from the ($\bar{2}01$) and (002) reflection intensities - and hence interference effects are minimal. None of the samples exhibited a sufficient number of characteristic reflections, for the Na-rich phase, to allow calculation of the unit cell parameters.

In order to estimate the bulk composition of the alkali feldspar separates, each sample was heated in a silica-glass tube at 990°C for three days. At the end

TABLE III

Sample #	Phase	Potassic Phase				Sodic Phase	
		Est. Or Wt%	degrees 2θ			Est. Ab Wt%	degrees 2θ 201
			201	060	204		
1	1	89.0	21.034				
2	1	88.5	21.039	41.714	50.612	99.5	22.041
3	1	90.0	21.014	41.705	50.669	98.0	22.018
4	1	89.0	21.030	41.661	50.706	95.5	21.985
5	2G	91.5	20.996	41.709	50.692	99.0	22.037
6	2G	89.0	21.034	41.687	50.673	97.0	21.998
7	2G	88.0	21.037	41.696	50.641		
8	2G	2 alkali feldspars present					
9	2C	89.0	21.029	41.676	50.659	97.0	22.001
10	2C	91.0	21.009	41.686	50.644	97.0	21.999
11	2C	89.0	21.026	41.701	50.667	98.0	22.019
12	2C	88.0	21.038	41.701	50.673		
13	2C	89.5	21.019	41.674	50.677	97.5	22.014
14	2LR	85.5	21.064	41.679	50.624		
15	2LR	86.5	21.052	41.684	50.677	98.5	22.029
16	2LR	85.0	21.071	41.681	50.684		
17	2LR	86.0	21.058	41.683	50.636		
18	2LR	89.0	21.026	41.693	50.657		
19	3	89.0	21.035	41.687	50.656	99.0	22.035
20	3	87.5	21.046	41.681	50.629		
21	3	89.5	21.021	41.684	50.647	98.5	22.029
22	4	91.0	21.004	41.686	50.646	98.0	22.020
23	4	89.5	21.024	41.676	50.668	97.5	22.015
24	4	2 alkali feldspars present					
25	4	89.0	21.029	41.654	50.682		
26	5	89.5	21.024	41.672	50.664		
27	5	86.5	21.055	41.679	50.652	97.5	22.014
28	5	86.0	21.061	41.729	50.639	96.0	21.976
29	5	85.5	21.067	41.708	50.634	98.5	22.027
30	5	87.5	21.046	41.676	50.672		
31	5	91.5	20.996	41.766	50.582	100.0	22.059
32	6	89.5	21.021	41.681	50.654		
33	6	90.5 ¹	21.011	41.681	50.642	100.0	22.051
34	6	89.5	21.021	41.693	50.672		
35	6	88.5	21.039	41.684	50.662		

TABLE IV UNIT CELL PARAMETERS FOR HOMOGENISED ALKALI FELDSPARS

Sample #	Phase	Wt% Or	Unit Cell Parameters							No. of lines used	Std. error (2σ)
			a(Å)	b(Å)	c(Å)	α	β	γ	V(Å) ³		
13 Homogenised	2C	83.0	8.540 ± .004	12.996 .003	7.200 .001	90°	115° 58.79' 1.75'	90°	718.41 .36	16	.017
29 Homogenised	5	73.5	8.513 ± .006	12.976 .004	7.199 .002	90°	116° 0.13' 1.71'	90°	714.85 .53	11	.017

of this period most samples showed only a single ($\bar{2}01$) reflection on diffractometer patterns, indicating that homogenisation was complete. Any samples exhibiting more than one ($\bar{2}01$) reflection were returned for further heating until no further change in the position of the $\bar{2}01$ reflection(s) was recorded. Unit cell parameters were determined for two of the homogenised samples using CaF_2 as an internal standard, (Table IV) and the position of the $\bar{2}01$ reflection was measured for the remainder (Table VI) using KBrO_3 (101 reflection at $20.215^\circ 2\theta$ $\text{CuK}\alpha$) as an internal standard.

c) Compositions of the Natural Feldspars

Wright and Stewart (1968) have shown that the a cell dimension, unit cell volume, and the position of the $\bar{2}01$ X-ray reflection of alkali feldspars show a direct correlation with composition which is independent of the structural state of the material. (Fig. 3). Thus, for those samples for which unit cell dimensions have been refined, the compositions of the K-rich phase have been estimated from the unit cell volume (Table II). Compositions for the remaining samples have been estimated from a knowledge of the position of the $\bar{2}01$ reflection. (Table VI).

Table V compares compositions estimated from unit

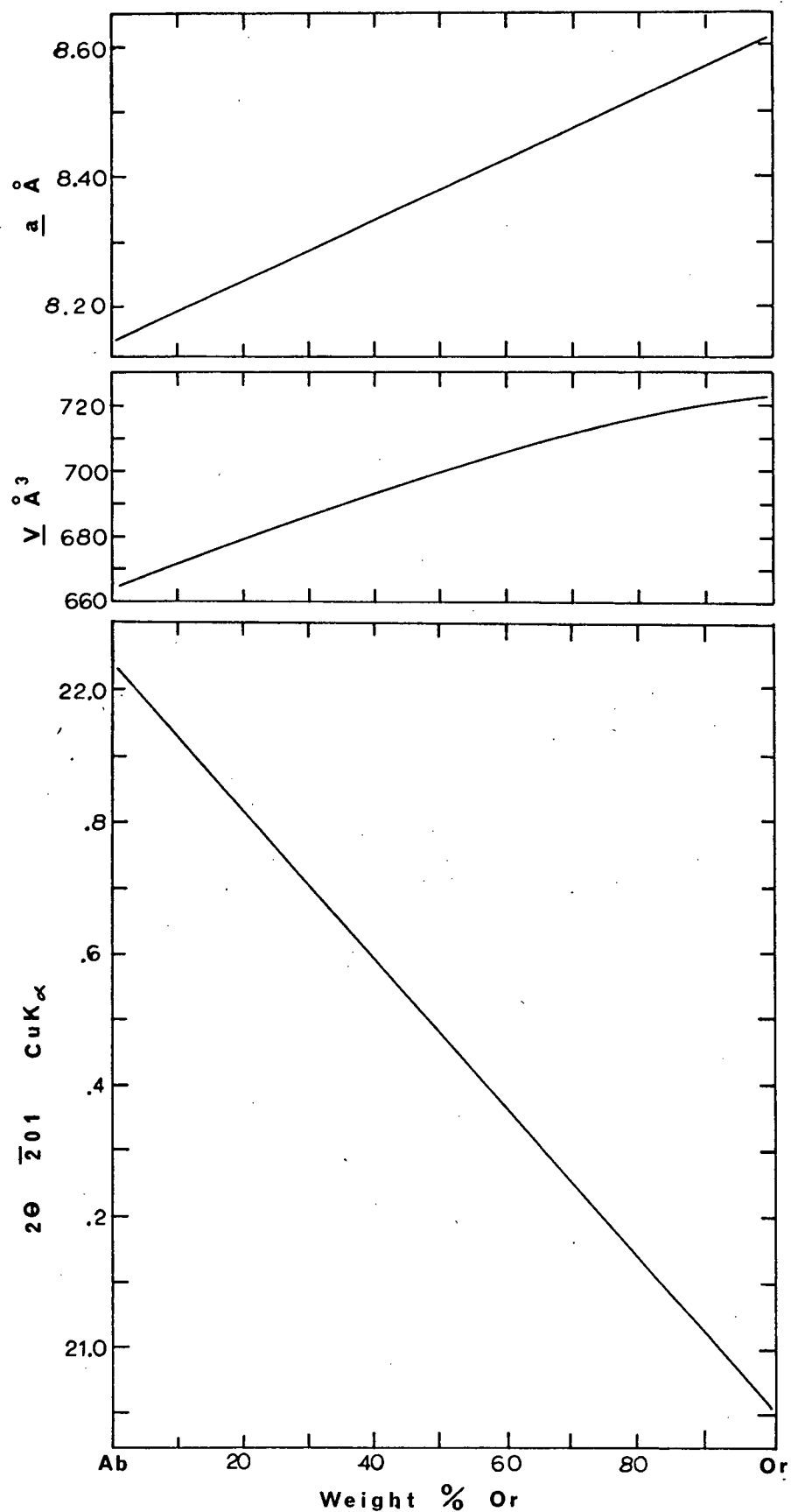


Fig. 3 Orthoclase content of alkali feldspars plotted as a function of the a cell dimension, unit cell volume and $2\theta \bar{2}01 \text{ CuK}\alpha$. Simplified from Wright and Stewart (1968) and Wright (1968).

cell volumes, a cell dimensions and $\bar{2}01$ X-ray diffraction reflections for the twelve 'refined' alkali feldspars. In general the estimates obtained from these three parameters agree within the $\pm 2\%$ accuracy claimed for the methods by Wright and Stewart (1968).

The samples investigated comprise K-rich phases whose compositions vary from 87 to 92 Wt% Or, and Na rich phases with compositions between 95 and 100 Wt% Ab. Because the error in measurement of composition is approximately ± 2 Wt% Or it can be stated that the alkali feldspars throughout the pluton have reached approximately the same stage of perthitic unmixing.

Although none of the samples exhibit any optical evidence of compositional zoning the $\bar{2}01$ diffraction peaks for the K-rich phase in several samples are very slightly skewed towards higher Or Wt% values, thus suggesting that slight zoning may in fact be present.

d) Structural States of the Natural Alkali Feldspars

The structural states of the K-rich phases of the natural perthites have been estimated from a knowledge of the b and c cell dimensions, or from the position of the (060) and ($\bar{2}04$) X-ray diffraction reflections. Figure 4 (simplified from Wright and Stewart) shows data

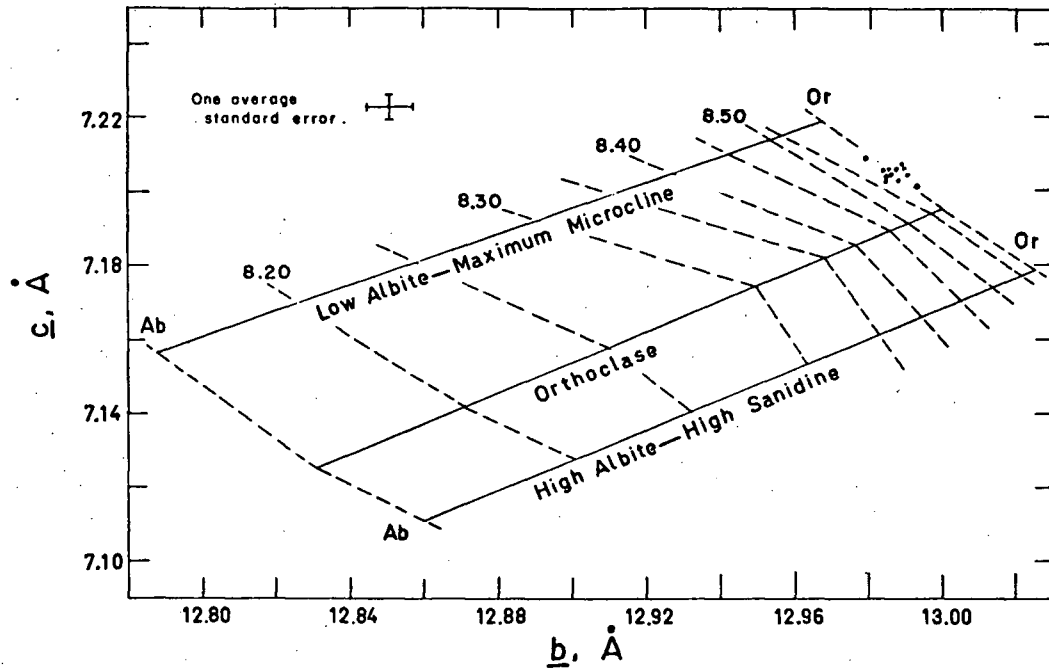


Fig. 4: Refined cell parameters for alkali feldspars from the Guichon Creek batholith plotted on a b - c plot simplified from Wright & Stewart (1968). Dashed lines represent contours for the a cell dimension.

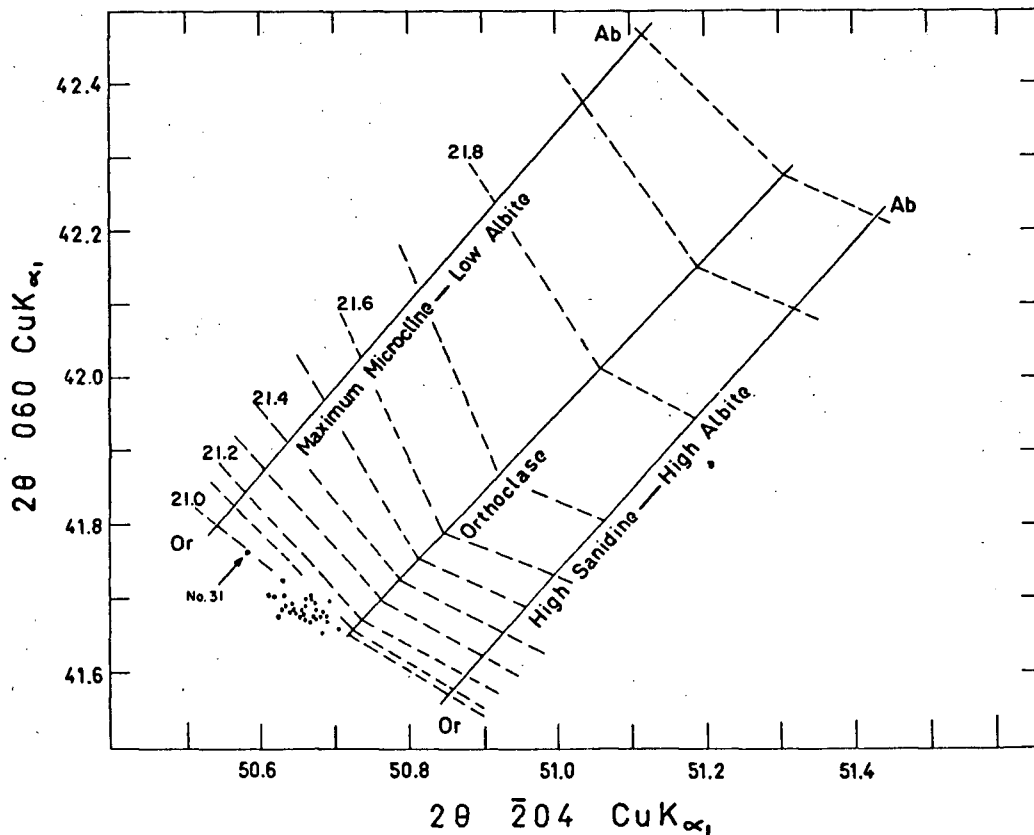


Fig. 5: Alkali feldspars from the Guichon Creek batholith plotted on a 060-204 plot simplified from Wright (1968). Dashed lines represent contours for 2θ 201.

TABLE V

Relation between estimated bulk compositions and degree of anomaly for
computer refined alkali feldspar

Sample	V(\AA) ³	a(Calc)(\AA)	a(est)(\AA)	Anomaly	201 obs.	Composition Wt% Or Estimated from			
						V	a(Calc)	a(est)	201 obs.
33	721.32	8.581	8.58	-	21.011	92.5	94	94	90.5
6	720.79	8.576	8.575	-	21.034	91.5	93	91	89.0
3	721.18	8.581	8.58	-	21.014	92.0	94	94	90.0
13	721.02	8.577	8.59	.012	21.019	92.0	93	96	89.5
19	721.13	8.580	8.60	.02	21.035	92.0	94	99	89.0
12	720.90	8.573	8.59	.02	21.038	91.5	92	96	88.0
29	719.79	8.562	8.59	.030	21.067	89.0	90	96	85.5
23	721.57	8.578	8.61	.032	21.024	93.0	93	99	89.5
22	721.97	8.584	8.62	.038	21.004	96.5	94	100	91.0
4	721.06	8.575	8.62	.045	21.030	92.0	93	100	89.0
17	719.60	8.555	8.61	.060	21.058	88.5	88	95	86.0
27	720.46	8.564	8.62	.060	21.055	90.5	90	100	86.5

for the 12 "refined" samples plotted on a b vs. c diagram. Similarly Figure 5 is a $^{\circ}2\theta$ (060) vs. $^{\circ}2\theta$ ($\bar{2}04$) plot of data for all the samples investigated.

When the b and c cell dimensions for any sample are plotted on Fig. 4 the a cell dimension may be estimated from the cross contours. For approximately half of the samples investigated the value for a so estimated does not agree with the a value calculated from the cell refinement. Wright and Stewart (1968) have described alkali feldspars in which a 'calculated' differs from a 'estimated' by more than .02 Å as having 'anomolous' cell dimensions. They suggest that in such cases the composition of the sample may be estimated from the cell volume, on the premise that the atoms will occupy the same volume regardless of the configuration of the unit cell. Furthermore, they state that the sample may be defined in terms of an 'apparent' structural state. Table V lists cell volumes, and calculated and estimated a cell parameters for the 'computer refined' samples investigated. The present study agrees with Wright and Stewart's observations that in all anomolous samples the a calculated values are lower than the a estimated values. However, Tilling (1968) has reported samples in which the reverse holds true. The anomalous

condition exhibited by such alkali feldspars would appear to be related to their perthitic nature and may be due to strains imposed on the structure during perthitic unmixing.

The Guichon batholith alkali feldspars plotted on Figures 4 and 5 lie within the orthoclase field between the orthoclase P50-56F of Wright and Stewart (1968) and the maximum microcline of Orville (1967). The only exception to this is sample #31 which plots on Fig. 5 within the intermediate microcline field. The sample is from a small intrusive mass on the western margin of the batholith, and has been tentatively correlated with the Witches Brook phase. The rock contains 26 vol% of medium to coarse grained microperthitic alkali feldspar which has a subhedral habit, and a bulk composition of 64Wt% Or. In addition, the rock contains 76 Wt% SiO_2 and appears to be the most highly differentiated of the samples studied. The X-ray diffractometer pattern for this sample contains no well defined $1\bar{3}1$ or $1\bar{3}\bar{1}$ reflections for the potassium rich phase. The reflections in the region between 29.25° and 30.50° 2θ $\text{CuK}\alpha$ are illustrated in Fig. 6. The higher intensity reflection with centre of symmetry at approximately 30.1° 2θ $\text{CuK}\alpha$ is most probably a composite reflection

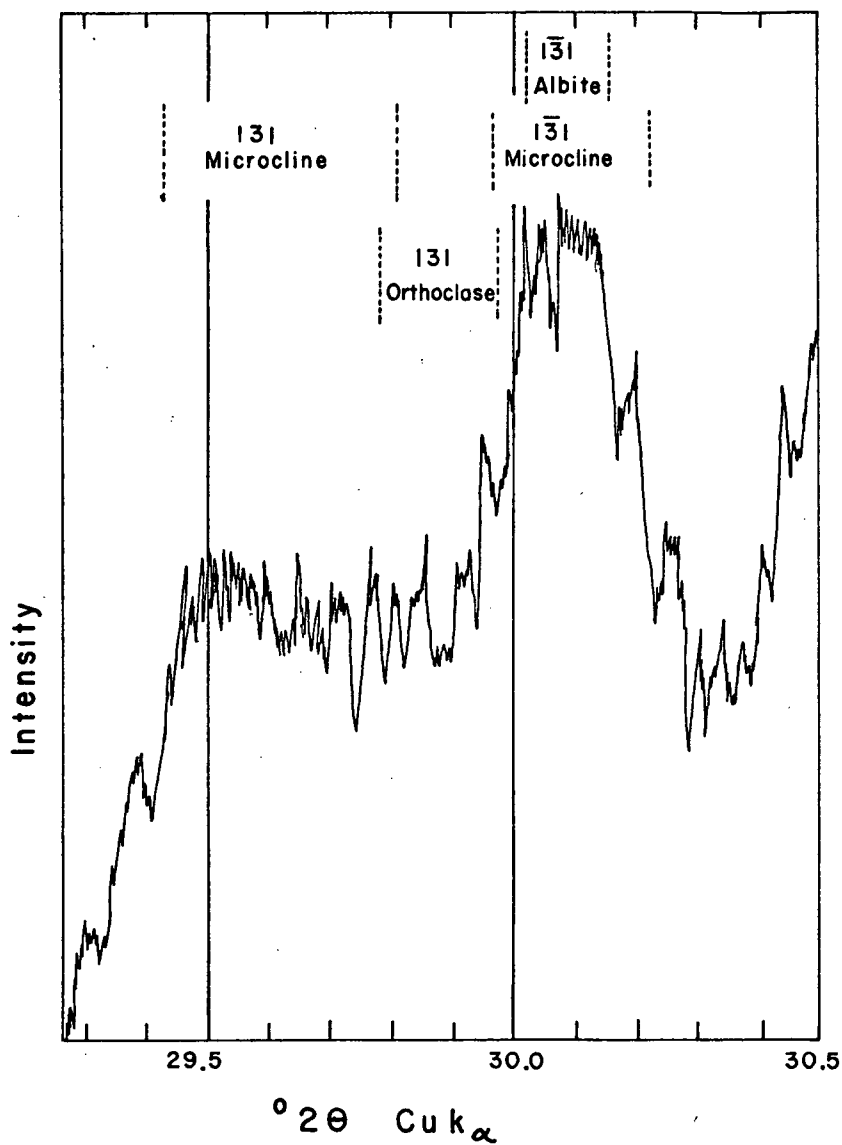


Fig. 6 X-ray diffraction pattern for sample 31 in the region of $30^{\circ} 2\theta \text{ CuK}\alpha$

Also shown are the ranges of potassic and sodic alkali feldspar reflections which may appear in this region. (From Wright and Stewart, 1968)

caused by the inference of the $1\bar{3}1$ albite reflection and a $1\bar{3}1$ microcline reflection. The very broad reflection extending from approximately 29.5° to 29.9° 2θ $\text{CuK}\alpha$ probably represents a 131 reflection from a triclinic potassium rich phase and there is a distinct possibility that a 131 reflection from a monoclinic potassium phase may also be represented here. This would indicate that the potassium rich phase of the perthite is present in a wide range of structural states. In contrast the 060 and $\bar{2}04$ reflections from the potassium rich phase in this sample are relatively sharp and well defined.

Smith and Mackenzie (1961) have suggested from theoretical considerations that as the Si-Al order of a perthitic alkali feldspar increases, so should the purity of the perthitic components. Tilling (1968) has observed a general increase in 'triclinicity' with increasingly albitic bulk compositions of perthitic alkali feldspars from the Rader Creek Pluton, Boulder Batholith, Montana. The compositions of the perthitic components in sample #31 approach closely the pure end member compositions and are very similar to the other samples from the Guichon Creek batholith. Sample #31

is unique however, because it is considerably more ordered with respect to Al and Si, and has a more sodic bulk composition than the other samples. Thus a greater degree of perthitic unmixing must have taken place in sample #31, and the consequently greater amount of diffusion of An and K ions may have allowed a higher degree of Si-Al ordering to take place.

Thus, with a single exception, the alkali feldspars from the Guichon batholith are orthoclase exhibiting approximately equivalent 'apparent' structural states. The slight scatter of data points on Figs. 4 and 5 most probably reflects, in large part, experimental errors and the anomalous nature of many of the samples. The equivalence in 'apparent' structural state of the alkali feldspars does not necessarily mean, however, that the temperature of their original crystallisation did not vary. The relative structural state of a monoclinic alkali feldspar is dependent on the degree of Al/Si ordering over the nonequivalent T_1 and T_2 tetrahedral sites. The ordering is achieved by diffusion, in the solid state, of Al into the more favourable T_1 sites, and the cooling history of the material will determine

the amount of time during which diffusion may take place. Therefore both the initial crystallisation temperature and the cooling history of the host rock will affect the final, relative structural state of an alkali feldspar.

e) Bulk Compositions of the Homogenised Alkali Feldspar

Table VI gives observed $^{2\theta}(\bar{2}01)$ for the homogenised samples and the corresponding estimated bulk compositions in Wt% Or. As may be seen alkali feldspar bulk compositions are generally in the range 71 to 86 Wt% with the exception of two samples from the Witches Brook Phase which have bulk compositions of 63 Wt% Or and 65 Wt% Or. There seems to be no regular variation of the alkali feldspar bulk compositions from one phase of the batholith to another, nor is there any correlation with the component oxide contents of the rock samples as derived from chemical estimates. (see Appendix 2)

TABLE VI

$^{\circ}2\theta$ values for $\bar{2}01$ reflections (CuK α radiation) and estimated bulk composition of homogenised alkali feldspars from the Guichon Creek batholith

Sample #	Phase	$^{\circ}2\theta(\bar{2}01)^*$	$^{\circ}2\theta$ Spread from 3 traces	$^+$ Estimated Wt% Or.
1	1	21.113	.005	81.5
2	1	21.124	.013	80.0
3	1	21.116	.003	81.
4	1	21.111	.003	82.
5	2G	21.216	.003	72
6	2G	21.146	.008	79.
7	2G	21.089	.002	84.
8	2G	21.169	.005	76.
9	2C	21.213	.005	72.
10	2C	21.119	.013	80.5
11	2C	21.120	.005	80.5
12	2C	21.082	.015	84.
13	2C	21.116	.010	81.
14	2LR	21.131	.010	79.5
15	2LR	21.123	.005	80.
16	2LR	21.141	.005	79.
17	2LR	21.132	.008	79.5
18	2LR	21.164	.008	77.
19	3	21.200	.010	73.5
20	3	21.096	.003	82.5
21	3	21.184	.013	75.
22	4	21.197	.005	73.5
23	4	21.144	.013	78.5
24	4	21.241	.010	70.
25	4	21.139	.003	79.
26	5	21.125	.005	80.
27	5	21.293	.008	65.5
28	5	21.150	.006	78.
29	5	21.204	.003	73.0
30	5	21.166	.008	76.5
31	5	21.319	.003	63.
32	6	21.152	.003	78.
33	6	21.231	.007	71.
34	6	21.179	.008	74.5
35	6	21.070	.005	85.

* $^{\circ}2\theta$ ($\bar{2}01$) values are averages of 3 diffractometer traces

+ Accuracy estimated at ± 2 Wt% Or.

IV Plagioclase Feldspars

a) Mode of Occurrence

Plagioclase occurs as subhedral or euhedral crystals in all phases of the batholith, and has an extremely variable grain size ranging from 4mm to less than 0.5mm. Albite or combined albite-carlsbad twinning is ubiquitous but pericline twinning is scarce. Normal and oscillatory zoning are common and patchy zoning is frequently present. Zoning is discussed more fully in the following section. Hornblende, magnetite and biotite inclusions are common, with biotite showing a slight tendency to be restricted to rim regions. In the Hybrid phase, and less commonly in the Highland Valley phase, pyroxene also appears as an inclusion and tends to be restricted to core regions. Intense alteration to a fine-grained colorless mica is especially common in the Hybrid phase and some alteration occurs in plagioclase core regions of almost all the samples studied.

b) Plagioclase Compositions and Zoning

Plagioclase compositions have been measured in thin-section using the perpendicular to 'a' method and a 4-axis universal stage. Universal stage measurements of $2V_z$ indicate that the structural states of the plagioclases vary from low to intermediate. Because

TABLE VII

Plagioclase compositions - see text for explanation

Sample #	Phase	Wt% An			Bulk composition	
		Core	Main Rim	Rim contact with Alkali feldspar	Wt % An Optical	X-Ray
1	1	47	36	36	43	44.0
2	1	35	28	heavy alteration	32	23.5
3	1	30	26	? heavy alteration	30	30.5
4	1	38	27	20	35	35.5
5	2G	36	27	none observed	31	25.5
6	2G	38	25	24	34	35.5
7	2G	38	27	20	32	28
8	2G	48	20	zero	30	24.0
9	2C	38	20	20	33	36
10	2C	36	20	zero	33	33
11	2C	36	26	26	33	33
12	2C	32	32	32	32	25.0
14	2LR	45	25	myrmekitic	39	32.0
15	2LR	41	24	24	33	32.0
16	2LR	39	25	20	33	33
17	2LR	31	20	20	28	27.5
18	2LR	32	20	20	28	31.5
19	3	33	20	zero	30	29.0
20	3	32	20	zero	27	28.5
21	3	27	20	zero	29	29.0
22	4	36	18	18	31	32.0
23	4	38	20	zero	28	27.5
24	4	38	20	zero	28	29.5
25	4	38	20	zero	30	31.5
26	5	48	20	zero	35	26.5
27	5	36	20	zero	28	27.5
28	5	29	20	zero	27	26.5
29	5	33	20	zero	28	28.0
30	5	40	20	zero	27	23.0
31	5	24	7	7 or zero	12	11.0
32	6	38	20	zero	28	28.5
33	6	32	20	20	28	27.5
34	6	34	20	zero	30	29.5
35	6	28	16	zero	24	23.5

the plagioclase exhibit considerable compositional zoning it is rather difficult to estimate bulk compositions. Because of this difficulty X-ray diffractometer patterns were obtained for all the samples, with six oscillations being made in the range 29° to $33^{\circ} 2\theta$ using $\text{CuK}\alpha$ radiation. The separation of the (131) and $(1\bar{3}1)$ peaks was measured and the average value for each sample compared to the 'low' plagioclase curve of Smith (1956). For 75% of the samples investigated the average composition from the diffractometer method agrees to within 2 Wt% An with the average value estimated by optical examination. For the remaining samples the diffractometer averages are lower in An content and all these samples contain plagioclases with strongly sericitised core regions. In such cases the average or bulk composition finally accepted was that obtained by optical examination. Table VII lists compositional ranges and optical and X-ray diffractometer estimates of average plagioclase compositions.

In general, core compositions are in the range An_{38} to An_{28} and it is only in the Witches Brook phase that this range is exceeded - An_{52} to An_{20} . Plagioclases from the Hybrid phase and from the Guichon variety of the Highland Valley phase have rim compositions averaging

An₂₇ whilst all the other samples investigated have rim compositions of approximately An₂₀.

Many of the samples exhibit poikilitic alkali feldspar in contact with subhedral-euhedral plagioclase. In such cases the alkali feldspar commonly occupies embayments into the plagioclase, (Plates 1 and 2) which suggests that resorption of plagioclase was taking place during the final stages of crystallisation in these samples. Furthermore, a very thin rim of albite occurs within the plagioclase, paralleling the resorbed outline of the crystal. (Plate 3) Two alternative hypotheses may be put forward to account for the presence of these albite rims:

(i) It is possible that, during resorption of the plagioclase, calcium may have been diffusing out of the plagioclase rim more rapidly than sodium. Late stage magmatic liquid in granitic rocks is commonly believed to be enriched in sodium and potassium relative to calcium. Therefore the composition gradient between late magmatic liquid and plagioclase crystals would be greater for calcium than for sodium, and hence more rapid diffusion of the calcium rich component out of the plagioclase is to be expected. The albite rims appear to have diffuse inner edges, which may support the diffusion hypothesis.



Plate 1 Partially resorbed plagioclase enclosed within poikilitic alkali feldspar. Sample #11. Chataway variety. Crossed nicols, x 30.

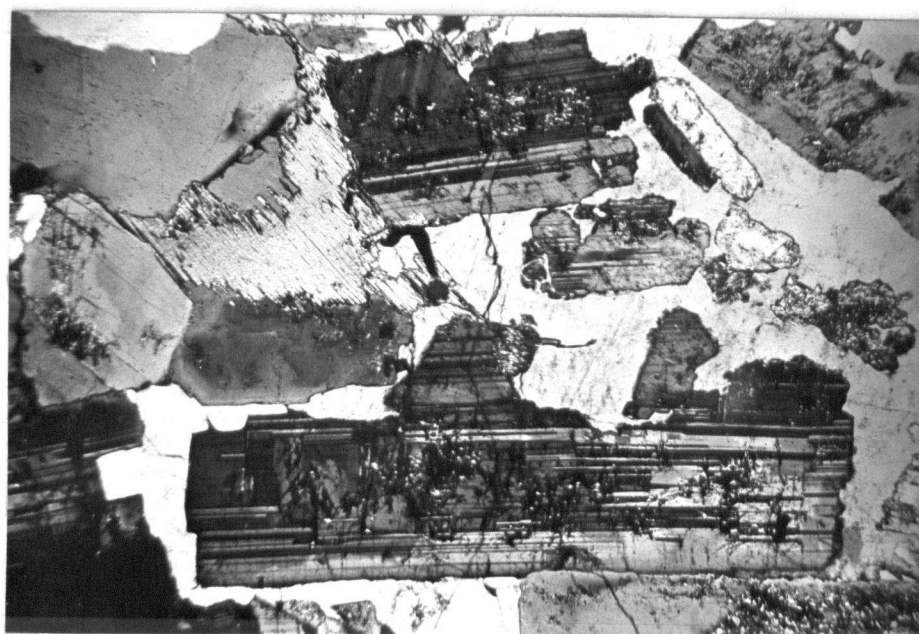


Plate 2 Partially resorbed plagioclase enclosed within poikilitic alkali feldspar. Sample #10. Chataway variety. Crossed nicols, x 30.

However, the thinness of the rims prevents a close study of this feature.

(ii) Bowen and Tuttle 1958 have suggested that albite rims on orthoclase-rich alkali feldspars may be the result of diffusion of the albite component to crystal margins during perthitic unmixing. This does not seem to be a very likely explanation in the present samples, however, because of the relatively fine scale of the associated perthitic lamellae. In addition, the albite rims are optically continuous with the plagioclase rather than with the alkali feldspars.

Late stage resorption of plagioclase has been explained by Tuttle and Bowen (1958) with reference to the system $\text{NaAlSi}_3\text{O}_8 - \text{KAlSi}_3\text{O}_8 - \text{CaAl}_2\text{Si}_2\text{O}_8$. In Fig. 7 the line ABC represents the limit of feldspar solid solution in this system and the line DEF is a single field boundary corresponding to liquid compositions which are in equilibrium with two feldspars at 1 kb water vapour pressure (James and Hamilton 1969). Strongly fractionated liquids which crystallised plagioclase at an early stage may eventually enter the field BEF, at which time plagioclase resorption and replacement by alkali feldspar may take place. Sample #31 represents a highly fractionated magmatic liquid which initially crystallised

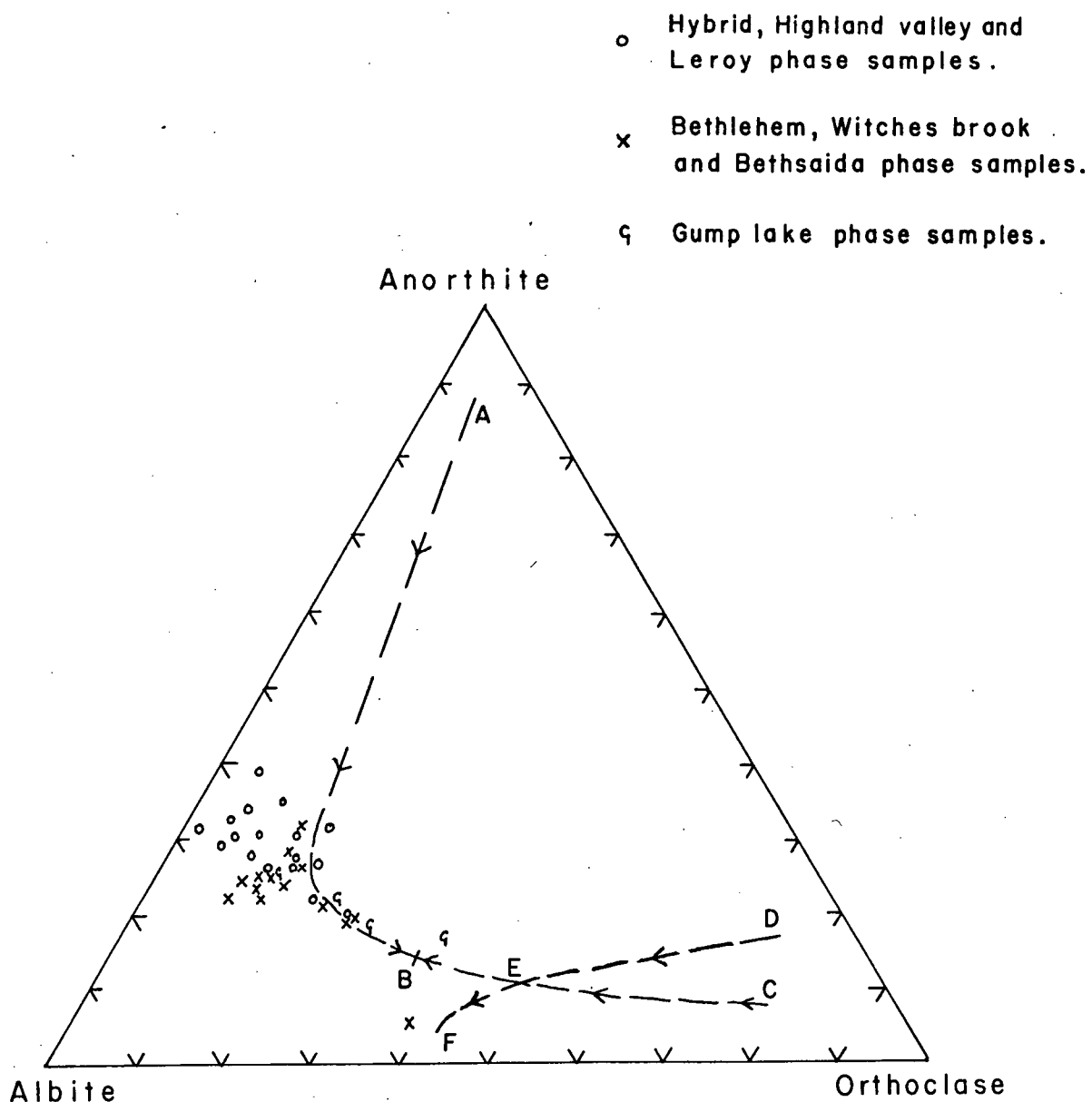


Fig. 7 . Modal feldspar constituents of the Guichon Creek batholith samples recalculated to 100% An+Ab+Or . ABC represents the limit of ternary solid solution in natural feldspars . DEF is the boundary curve separating the fields of plagioclase and alkali feldspar .

plagioclase feldspar An_{22} . This plagioclase rapidly became out of equilibrium with the magmatic liquid and was consequently partially resorbed and replaced by an alkali feldspar Or_{64} . Thus #31 consists of an equigranular mosaic of quartz, alkali feldspar and crystals with partially resorbed plagioclase cores and alkali feldspar mantles.

Although plagioclase compositions show very little variation throughout the batholith, the nature of the zonation is significant and divides the phases into two major groups. Thus plagioclases from the Hybrid and Highland Valley phases exhibit only normal zoning with superimposed patchy zoning, whilst those from the Bethlehem and Bethsaida phases have delicately oscillatory zoned cores and normally zoned rims. The change from core to rim regions is in all cases gradational through progressive normal zoning. Plagioclases from the Gump Lake phase exhibit a zoning scheme intermediate between the two previously described, in that cores may have three or four very broad oscillatory zones followed continuously by a normally zoned rim. Samples from Northcote's Witches Brook phase may exhibit either or both of the schemes, suggesting that some of these samples are related to the Highland



Plate 3 Partially resorbed, oscillatory zoned plagioclase enclosed within poikilitic, perthitic alkali feldspar. Note the albitic rim to the plagioclase. Sample #25, Bethlehem phase. Crossed nicols, x 30.

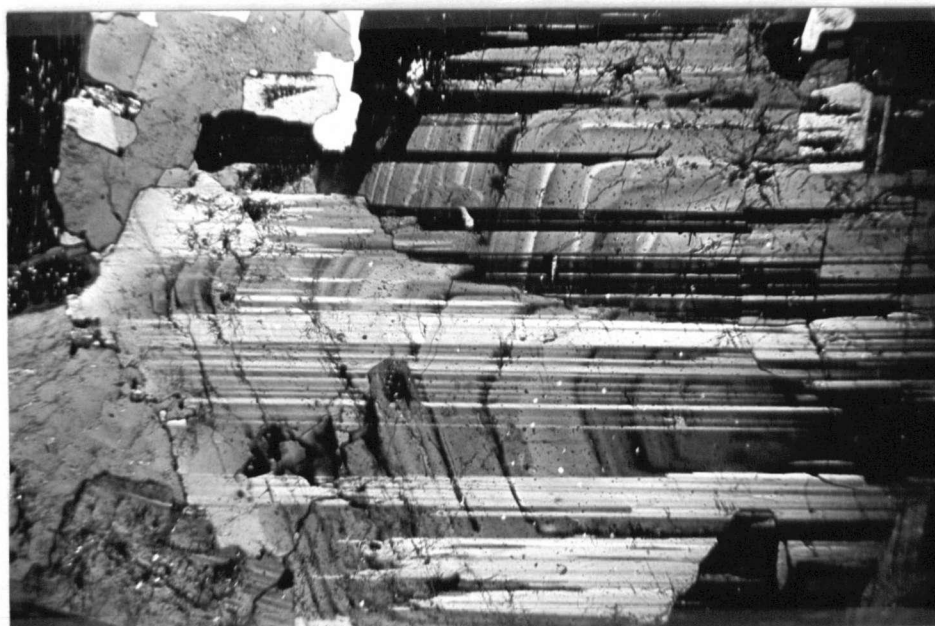
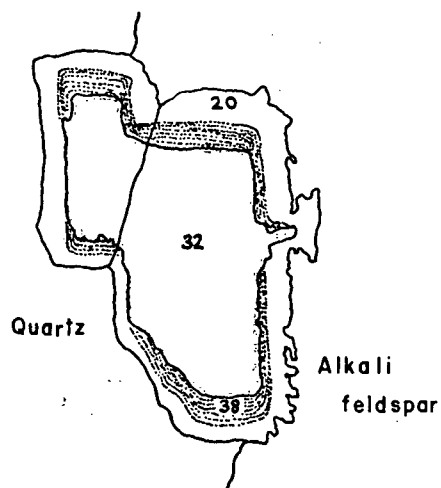


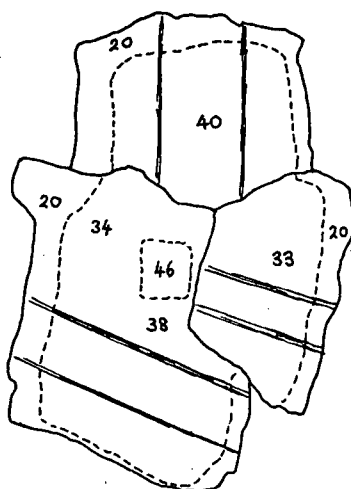
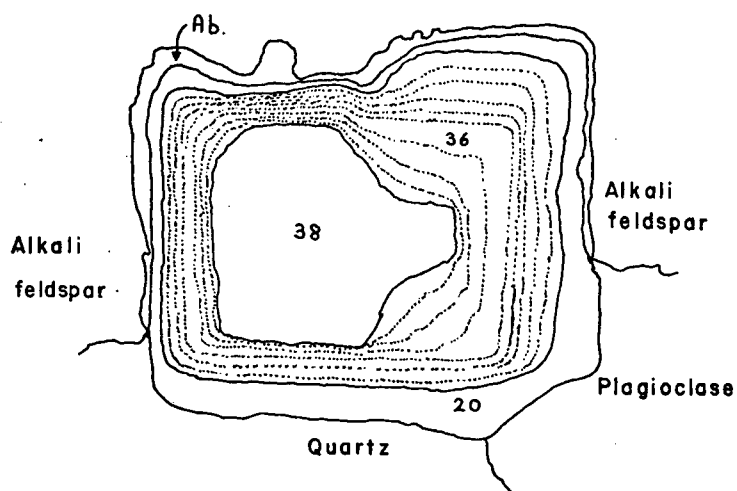
Plate 4 Oscillatory zoning in plagioclase. Sample #34. Bethsaida phase. Crossed nicols, x 30.

Fig. 8 Plagioclase zoning schemes.



Sample 27
Witches Brook phase.

Sample 25
Bethlehem phase.



Sample 8
Guichon variety
Highland Valley phase.

0 0.5 1.0
Millimetres

Valley phase and others to the Bethlehem phase. Fig. 8 illustrates the nature of the zoning schemes. Sample #27 is particularly interesting in that it displays a homogenous core (An_{32}) similar to samples from the Highland Valley phase, which terminates in an absorption rind and is followed by a more basic oscillatory zoned inner rim An_{38} giving way to a normally zoned outer rim (An_{37-20}), a characteristic of the Bethlehem and later phases.

Normal zoning in plagioclase crystals is generally believed to result from non-reaction between crystals in the anorthite-albite solid solution series and magma during crystallisation in response to falling temperature. Such lack of reaction would seem likely for plagioclases of the Hybrid and Highland Valley phases which are believed to have crystallised under conditions of convective magma flow. Conversely the mechanisms leading to the development of delicate oscillatory zoning in plagioclases are imperfectly known. Vance (1957) has discussed the various theories. Basically the theories can be divided between those that invoke repeated variations of temperature, pressure and/or partial volatile pressure or require repeated relative movement of crystal and magma, and those based on the

diffusion supersaturation theory of Harloff (1927) as expanded by Hills (1936) and Bottinga et al (1966). The latter authors relate the degree of supersaturation in the magma immediately adjacent to the crystal-liquid interface to the mechanism of nucleation and the geometric configuration of that interface. The presence of a supersaturated layer immediately adjacent to the interface of oscillatory zoned bytownite crystals set in the glassy matrix of an oceanic basalt has been proven by Bottinga et al using an electron microprobe analyser. The theory requires that there be no relative movement between growing plagioclase crystals and the boundary layer in the magma immediately adjacent to the interface. Most of the oscillatory zoning observed in plagioclases from the Bethlehem and Bethsaida phases is of the regular, delicate type. If this type of zoning were due to variations of temperature or pressure within the magma chamber it would require that these variations be extremely regular in both timing and degree. For this reason the modified diffusion-supersaturation theory is considered by the present author to be the most viable explanation currently available for the presence of regular delicate oscillatory zoning in igneous plagioclases. Some of the Bethlehem phase plagioclase crystals do,

however, contain one or two slightly wider zones that have irregular outlines. It is possible that these zones may represent variations in volatile pressures accompanying intrusion of Witches Brook dyke phase.

Vance (1957) has discussed the origin of normally zoned rims succeeding oscillatory zoned cores in plagioclase crystals. He has suggested that the attainment of volatile saturation with consequent resurgent boiling may be sufficient to prevent the operation of the diffusion-supersaturation process and growth of oscillatory zoned plagioclase, thus causing the deposition of normally zoned rims. Piwinski (1968) has carried out melting experiments on granodiorite samples from the Sierra Nevada batholith and had determined compositions of feldspars coexisting with the melt at various temperatures. (Fig. 9) This study has shown that in the water saturated system, the plagioclase composition coexisting with the melt changes rapidly with initial slight increase in temperature. Further increases in temperature cause the rate of change of plagioclase composition to decrease markedly. The onset of rapidly changing plagioclase equilibrium compositions during crystallisation would probably tend to terminate the effectiveness of any slow diffusion process likely to

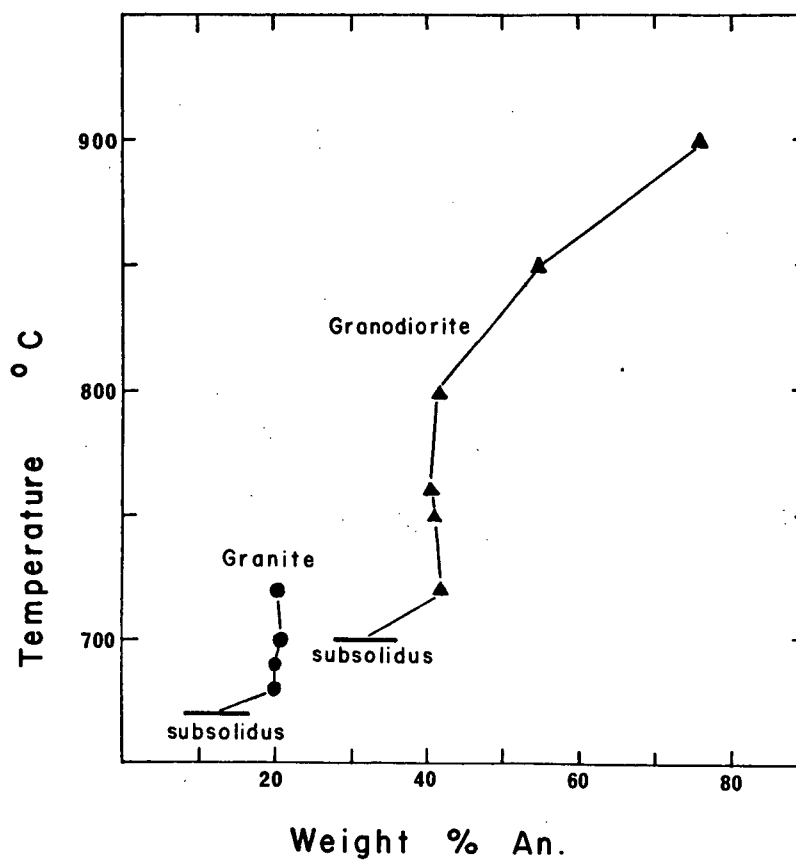


Fig. 9 Compositions of plagioclases in equilibrium with granitic melts as a function of temperature at 2 kb water pressure. (After Piwinski, 1968, p.560)

cause oscillatory zoning, thus causing the precipitation of normally zoned plagioclase. Textural evidence suggests that the Bethlehem and Bethsaida phases crystallised under conditions of higher volatile pressures than had previously existed. Piwinski's experimental data are therefore probably applicable to plagioclase crystallisation in these phases and the hypothesis based on his study is presented as an alternative to Vance's suggestion.

The unique plagioclase zoning scheme present in two of the Witches Brook phase samples, (#27 and #26) is not easily explained. The partially resorbed, normally zoned cores of these plagioclases suggest affinities to the Highland Valley phase, whilst the outer zoning schemes are identical to those present in Bethlehem phase plagioclases. Northcote (1969) has suggested that the Witches Brook phase may be a dyke phase associated with the major Bethlehem phase. If such is the case then the resorbed plagioclase cores of samples #27 and #26 may be xenocrysts of earlier phases which were mantled by typical Bethlehem phase material, prior to being intruded as dykes of the Witches Brook type. The lack of such xenocrysts within the major Bethlehem phase rocks may be due to the fact that more complete assimilation was possible deeper within the main chamber.

V Biotites

a) Mode of Occurrence

Biotite is present in all of the samples studied from the batholith. The amount of biotite tends to decrease with increasing silica content of the host rock (Fig 10). In rocks with less than 65 Wt% SiO_2 content biotite is accompanied by both pyroxene and hornblende. Biotite and hornblende occur in approximately equal amounts in those rocks with SiO_2 contents between 65 Wt% and 70 Wt%, and biotite is the dominant mafic mineral in more siliceous rocks. In rocks containing greater than 75 Wt% SiO_2 biotite is the only ferromagnesian silicate present. In addition, quartz, plagioclase, alkali feldspar and magnetite are present in all the samples but muscovite is entirely absent.

Biotite generally occurs as ragged, subhedral to euhedral crystals and exhibits a wide range in grain size. Some of the coarse-grained samples contain large, euhedral, poikilitic biotites with plagioclase, quartz and magnetite occurring commonly as inclusions. Only in the Hybrid phase does biotite exhibit a tendency to rim or replace pyroxene and hornblende, in all other phases biotite and hornblende coexist without replacement.

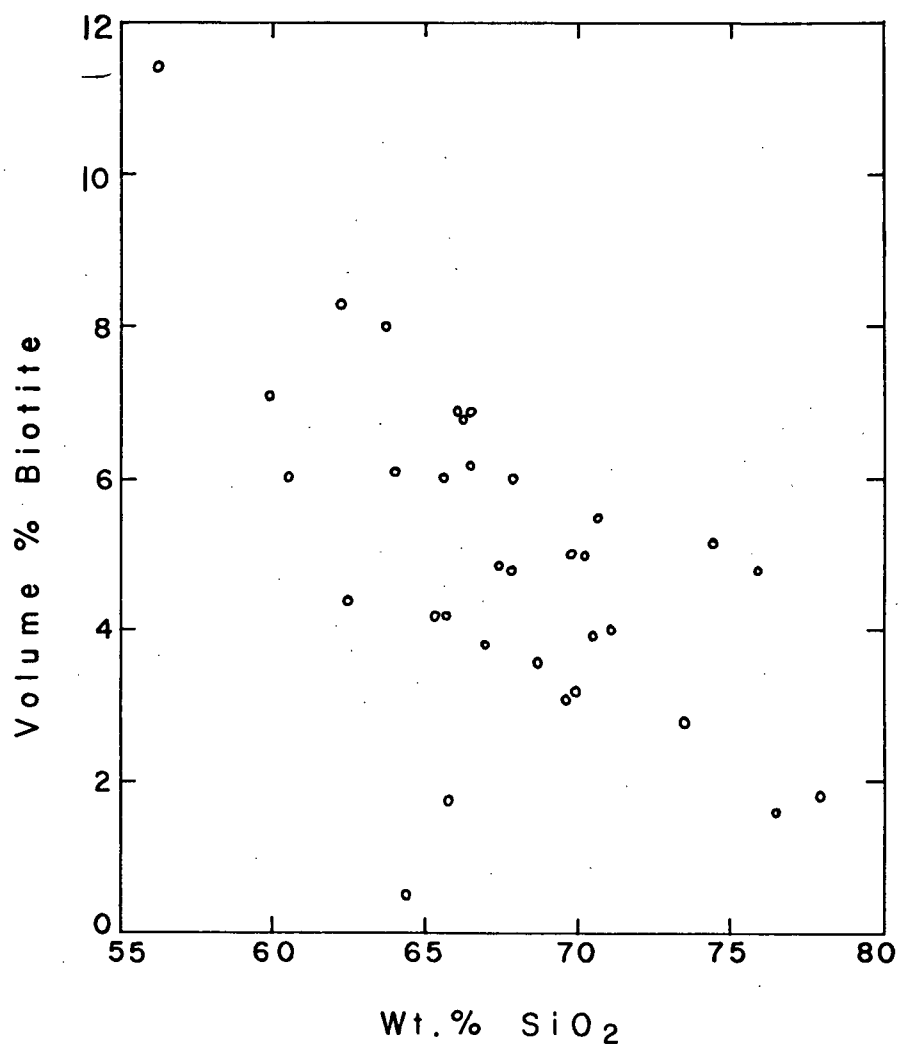


Fig.10. Relation between abundance of biotite and silica content of host rock.

The type of inclusions present in all of the biotites suggest that biotite started to crystallise during the simultaneous crystallisation of plagioclase and quartz, but prior to the separation of alkali feldspar.

Chloritic alteration of biotites is insignificant in the majority of the samples but up to about 50% chloritisation occurs in a few samples.

b) Method of Study

Biotite micas exhibit a large range of possible chemical substitutions within the crystal structure. Thus Al^{3+} may replace Si^{4+} in the tetrahedral layer, Ca, Na, Ba, Rb etc may substitute as interlayer cations in place of K., and OH^- anions may be replaced by Cl^- or F^- . The most petrogenetically important substitutions however occur in the octahedral layer where Mg^{2+} may be replaced by Fe^{2+} , Fe^{3+} , Al^{3+} , Ti^{3+} and Mn^{2+} . Differences in physical properties of the biotites are caused by the wide range of possible chemical substitution. It is not surprising therefore that attempts to correlate changes in physical properties with the variation in concentration of a single element or simple element ratio have been largely unsuccessful. (c.f. Rimsaite 1967).

The present author has attempted to make estimates

of the percentage of total octahedral iron group metals present in biotites from the Guichon Batholith using Gower's (1957) X-ray diffractometer method. The results have shown that variation in the degree of preferred orientation of the sample may introduce as much as 10% variation in the estimated percentage of total octahedral iron group metals, (Table VIII) when intensity ratios I_{004}/I_{005} are related to Rimsaite's Fig 11 (1957 p.37). The study was thus discontinued in favour of more direct chemical analysis.

Sample #	Sample Preparation	I_{004}/I_{005}	% Fe oct.
A.1	Coarse grind - slurry mount	.684	28
A.2	Fine grind - slurry mount	.570	22
B.1	Fine grind - slurry mount	.661	27
B.2	Fine grind - slurry mount	.937	40
B.3	Fine grind - centrifuged	.848	36
B.4	Fine grind - centrifuged	.822	35
C.1	Fine grind - slurry mount	.827	35
C.2	Fine grind - slurry mount	.741	31

Table VIII Observed intensity ratio I_{004}/I_{005} for 3 biotite samples as a function of sample preparation

Any form of standard chemical analysis technique of mineral concentrates suffers from the fact that it is sometimes impossible to obtain a completely pure sample. In analysis of biotite concentrates, admixtures of iron

oxide, chlorite, amphibole and inclusions of zircon, sphene, rutile, apatite and quartz may introduce large and unknown errors. For this reason, the electron-microprobe has been used for partial analyses of the biotites from the Guichon batholith. The use of this instrument has the added advantage that only small amounts of the sample are required. Biotite mineral concentrates for approximately half of the samples studied had already been produced by K.E. Northcote for use in K/Ar age determinations. The present author is grateful to Dr. Northcote and to Dr. W.H. White for permission to use these concentrates in the present study. Biotites from the remaining samples were concentrated by sieving of crushed rock followed by hand picking of the +40 mesh fraction. Details of the experimental techniques employed in the electron microprobe analyses and a discussion of the errors involved in the method are presented in Appendix 3.

c) Discussion of Results

The results of the partial analyses of 14 biotite samples from the Guichon batholith are given in Table IX. Results are given in terms of Wt% Mg and Fe since it is not possible to distinguish various valence states with the electron microprobe. For this reason the results for

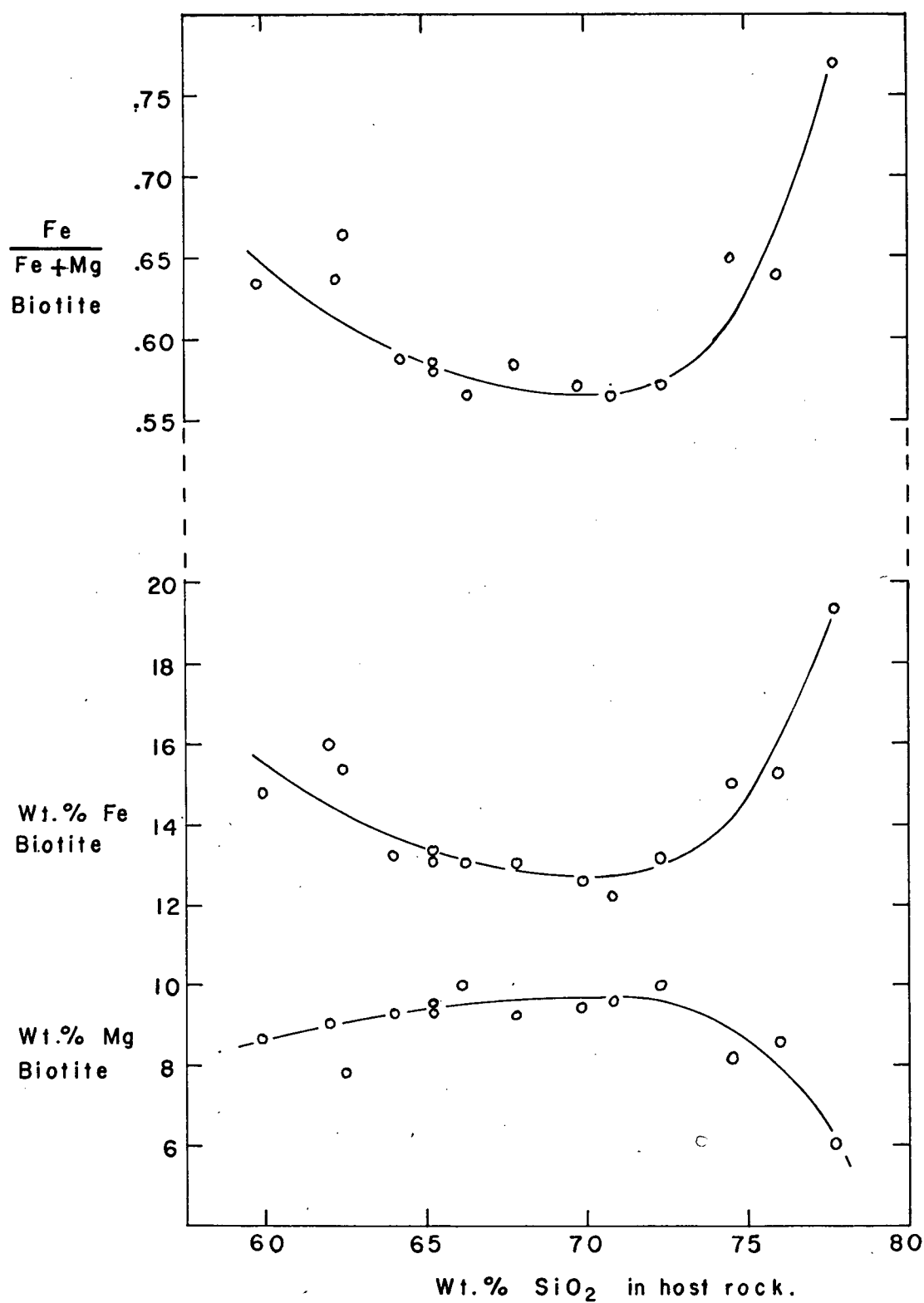


Fig.II: Biotite compositions as a function of the silica content of the host rock .

Sample #	Wt% Mg microprobe	σ Mg Wt% \pm	Wt% Fe microprobe	σ Fe Wt% \pm
31	6.0	.30	19.5	.25
14	7.8	.35	15.5	.10
19	8.1	.25	15.1	.20
20	8.6	.25	15.3	.25
6	8.6	.50	14.8	.70
2	9.1	.25	16.0	.40
23	9.2	.30	13.0	.30
4	9.3	.20	13.3	.10
29	9.4	.30	12.6	.20
15	9.4	.35	13.3	.05
9	9.4	.50	12.9	.10
34	9.5	.20	12.4	.20
34 (Dup)	9.7	.35	12.2	.25
11	10.0	.30	13.0	.10
35	10.0	.35	13.3	.10

Table IX Results of partial electron-microprobe analysis of biotites from the Guichon Creek batholith. σ (one standard deviation) is a function of sample inhomogeneity, surface roughness and the statistical variation of X-ray generation.
(see Appendix 3)

iron must be regarded as total iron ($\text{Fe}^{2+} + \text{Fe}^{3+}$).

Relative errors in analyses; taking into account experimental errors, the statistical variation in X-ray generation, and sample inhomogeneity; are estimated as ± 0.35 Wt% Mg and ± 0.25 Wt% Fe. No regular compositional zoning was observed in any of the samples studied.

There is a regular variation in the iron and magnesium contents of the biotites with increasing acidity of the host rock. Thus for the hornblende-bearing samples there is a decrease in the $\text{Fe}/(\text{Fe} + \text{Mg})$ ratio of the biotites with increasing content of SiO_2 in the host rock (Fig 11). This trend is reversed in those samples that contain biotite as the only ferromagnesian silicate mineral, i.e. those rocks containing greater than 73 Wt% SiO_2 . The observed biotite compositional trends are remarkably similar to those that exist within the Ben Nevis, Scotland, igneous complex; as reported by Haslam (1968). Furthermore, in the Ben Nevis complex, the hornblendes and clinopyroxenes exhibit compositional variations that are exactly analogous to those of the coexisting biotites. Haslam has emphasised that this observed trend of decreasing $\text{Fe}/(\text{Fe} + \text{Mg})$ ratios in ferromagnesian silicates with increasing differentiation of the host rock is the reverse of what might be suggested

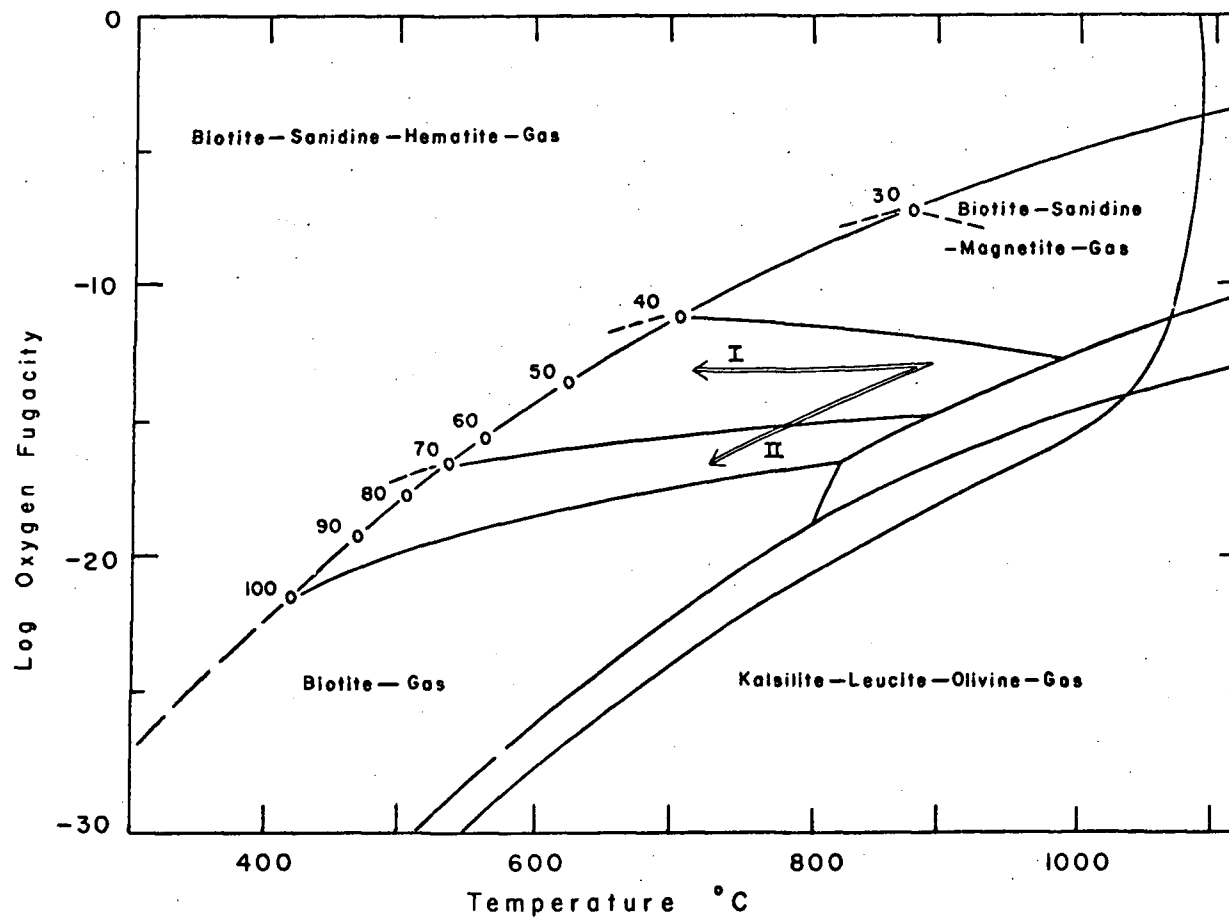


Fig. 12 Stability of biotites as a function of fO_2 and temperature at 2070 bars total pressure. Subhorizontal lines represent contours of constant $100 \text{ Fe}/(\text{Fe}+\text{Mg})$ values. Arrows labelled I and II represent oxidising and reducing trends in crystallising magmas. Diagram from Wones and Eugster, (1965)

by the results of experimental studies of synthetic systems. The factors which may contribute to this reversal include the partial pressures of oxygen and water and the total pressures operative, and the phase assemblages present.

Wones and Eugster (1965) have studied the compositional variation of synthetic biotites crystallised at variable oxygen fugacities. Fig 12 is a reproduction of Wones and Eugster's Fig 13 (1965, p.1254) and shows the stability of biotites as a function of fO_2 and temperature at a total pressure of 2070 bars. This diagram represents unusual bulk compositions because biotites are much more commonly associated with amphiboles and pyroxenes than with olivines. Wones and Eugster emphasise the fact that extrapolations from Fig. 12 to assemblages containing biotite and amphibole + pyroxene are unreliable. The two trend lines labelled I and II on Fig 12 represent the changing conditions expected during hypothetical crystallisation of two magmas. Trend I represents a magma which, during crystallisation and cooling, becomes saturated in H_2O , reacts with that component, and loses hydrogen to the environment. Under such conditions biotite compositions will remain essentially constant. Trend II represents

a magma that is 'buffered' by the mineral assemblage that it contains. Thus with falling temperature, fO_2 also decreases and biotite compositions will become consecutively more iron rich.

Evidence will be presented in Chapter VI which suggests that crystallisation of the Guichon batholith occurred under conditions of progressively increasing volatile pressures. In such a case the possibility exists that oxygen fugacities may also have been increasing due to reaction between water and magma and the loss of hydrogen to the environment. This would explain the observed slight progressive decreases in Fe/Fe + Mg ratios in biotites with progressive consolidation of the magma. The reversal of the trend that occurs at 73 Wt% SiO_2 of the host rock in Fig 11 also corresponds to a change in the mineral assemblage present, where biotite becomes the only ferromagnesian silicate present. It is possible that the new mineral assemblage may have a 'buffering' effect on the prevailing oxygen fugacities - an effect that was not present with the previously existing mineral assemblage. If this is correct then the oxygen fugacity would decrease with decreasing temperature and the observed rapid increase in the Fe/Fe + Mg ratio in biotites would

be produced. It is therefore suggested that the mineral assemblage and the partial pressures of volatiles that existed during crystallisation of that assemblage may both have had an effect on the composition of the biotites crystallising from the magma.

The discussion of biotite crystallisation in the Guichon batholith has, of necessity, been purely qualitative. Wones and Eugster (1965) have published data that allow quantitative estimates to be made of the independent intensive parameters, temperature, fugacity of H_2O , and fugacity of oxygen, which were operative during crystallisation of the assemblage biotite + sanidine + magnetite. The common assemblages present in the Guichon batholith samples, however, include hornblende, plagioclase, quartz \pm clinopyroxene, pyrite or other sulphides, sphene apatite and zircon, in addition to biotite, alkali feldspar and magnetite. Furthermore in any calculation of the intensive variables operative during crystallisation, the activity of the $KFe_3AlSi_3O_{10}(OH)$ component is a critical factor. The data presently available for the Guichon batholith biotites does not allow an estimate of this parameter because of the lack of any quantitative data on the Fe^{3+}/Fe^{2+} ratio in the biotites. The evaluation of this

ratio by standard wet chemical analysis suffers from inaccuracies that are due to the presence of magnetite and/or chlorite as inclusions in the biotite.

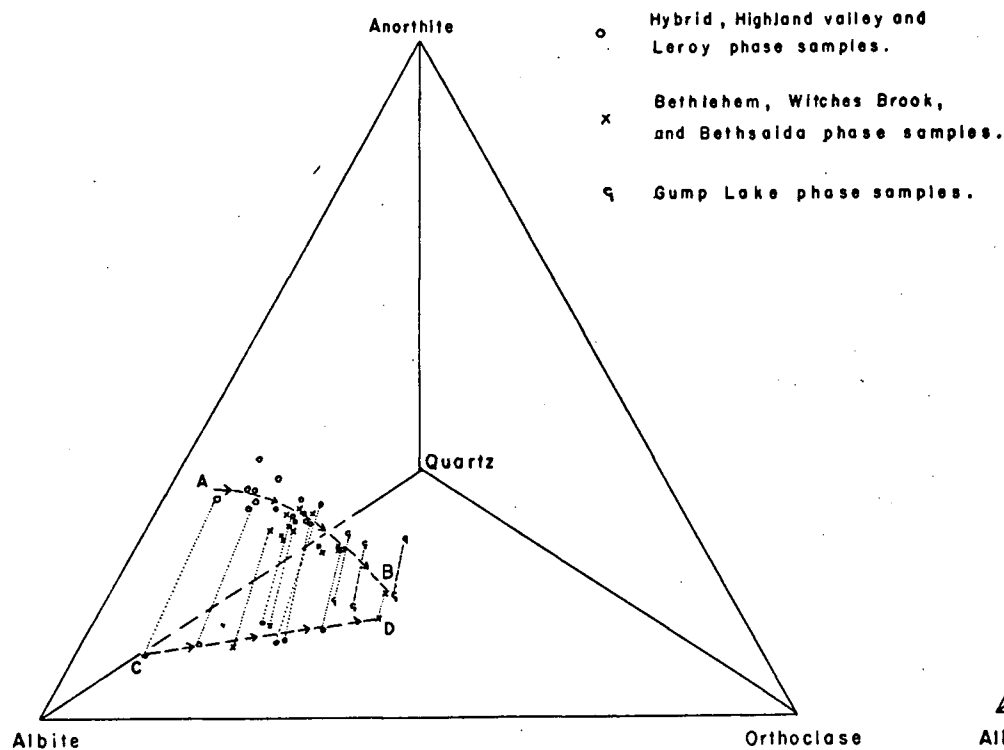


Fig. 13 a: Plot of modal quartz—orthoclase—albite—anorthite for the Guichon Creek batholith samples. A—B is the trend line for the samples in three dimensions. C—D is a projection of A—B onto the base of the tetrahedron from the anorthite corner.

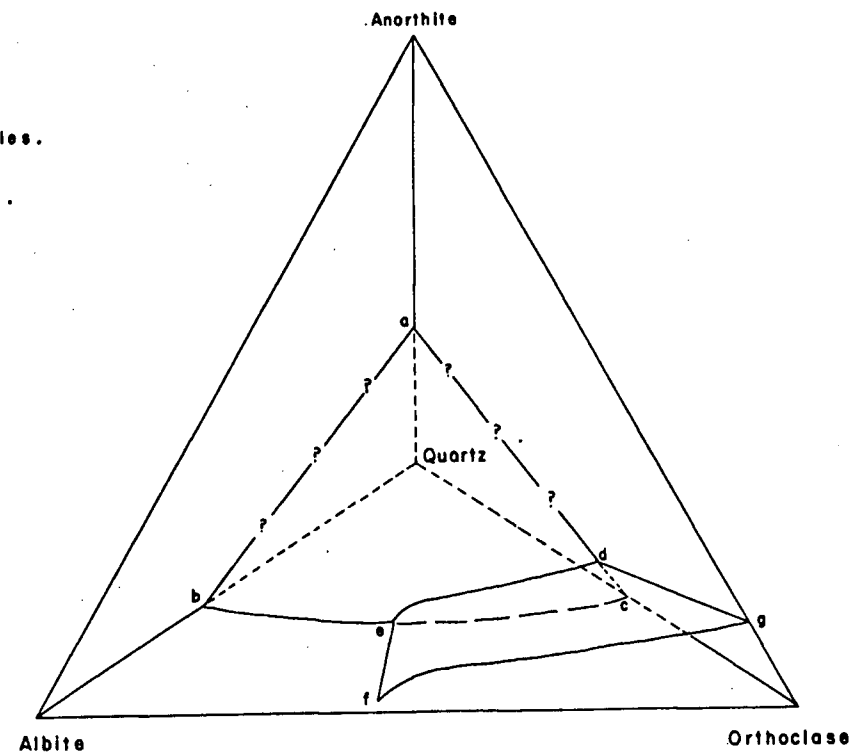


Fig. 13 b: Schematic phase diagram for the quaternary system Qz—Or—Ab—An. at 1 kilobar water vapour pressure.

VI Modal Analyses and Calculated Chemical Compositions

Modal analyses for approximately half of the samples investigated have been reported by Northcote (1969). For the remainder of the samples modal analyses were carried out on standard thin sections using a traversing point count microscope stage. For coarse-grained samples 500 points were counted in each thin section with a point spacing of 1mm, fine-grained samples were analysed with a point spacing of $\frac{1}{2}$ mm and 1000 points were counted. Modal analyses are presented in Appendix 2.

Fig 13a shows the mineralogical variation within the pluton expressed in terms of modal quartz, orthoclase, albite and anorthite recalculated to 100 Wt%. Within the 'granodiorite' tetrahedron of Fig 13a the samples, with the exception of those from the Gump Lake phase, all lie on the plane ABCD which intersects the Q, Or, Ab base of the tetrahedron in line CD. The line AB describes the trend of the gradually differentiating magma towards increasing quartz and orthoclase contents, decreasing plagioclase components and concomitant increase in the Ab/An ratio.

Fig 13b is a hypothetical phase diagram of the granodiorite system based partly on experimental investigations of the ternary systems that constitute the

faces of the tetrahedron. Phase relations in the system Ab-Or-Q have been studied at water vapour pressures from 0.5 to 10Kb by Tuttle and Bowen (1958) and Luth, Jahns and Tuttle (1964). Yoder (1967) investigated ternary compositions in the system Ab-An-Q at 5 kb water vapour pressure. The binary system An-Q has been studied at atmospheric pressure by Schairer and Bowen (1947) and at 1kb PH_2O by Stewart (1967). Preliminary data on the system An-Ab-Or have been published by Franco and Schairer (1951), Yoder, Stewart and Smith (1957) and James and Hamilton (1969). Similarly experimental results in the system An-Ab-Or-Q- H_2O have been published by Von. Platen (1965) and by James and Hamilton (1969). The curved surface abcd within the tetrahedron of Fig 13b separates regions of compositions first crystallising feldspar, from those first crystallising quartz. Compositions lying on this plane will be in equilibrium with both of the minerals whose regions it separates. The plane defg similarly separates the two feldspar regions; above this plane plagioclase is the primary phase, and below it alkali feldspar is the primary phase. The two surfaces intersect to form a line along which liquids are in equilibrium with plagioclase + alkali feldspar + silica + vapour.

The sequence of rock compositions from the Hybrid

phase, through the Highland Valley phase to the LeRoy granodiorite occupy successively more differentiated positions along the trend A-B in Fig 13. Textural evidence from these rocks indicates that plagioclase was the first felsic mineral to crystallise and that it was followed at a much later stage by quartz, and finally by alkali feldspar which is conspicuously interstitial or poikilitic. This is exactly the sequence of felsic crystallisation that would be predicted by Fig 13.

Rock compositions from the Gump Lake phase do not lie on the general trend surface ABCD in Fig 13 but are displaced towards the quartz corner of the tetrahedron. Northcote (1969) has suggested that the Gump Lake phase may not be related genetically to the rest of the Guichon batholith and that it may be an offshoot of the central Nicola batholith which lies to the east. The relations shown in Fig 13 tend to support Northcote's suggestion. Plagioclase and quartz crystals in the Gump Lake phase tend to be equidimensional suggesting that they perhaps crystallised almost simultaneously, whilst alkali feldspar is either institial or poikilitic. The Gump Lake samples plot on Fig 13b approximately on the plagioclase - quartz surface some way above the plagioclase - quartz - orthoclase equilibrium line,

which supports the proposed crystallisation sequence.

The samples from the Bethlehem and Bethsaida phases plot on Fig 13 in a position that lies within the general trend and is not radically different from that of the Highland Valley phase, but which indicates a slight enrichment in albite. LeRoy granodiorite samples plot on Fig 13 in a position which indicates that they are more differentiated than the bulk of the Bethlehem and Bethsaida phase samples. This tends to confirm Northcote's (1969) suggestion that the LeRoy granodiorite dyke phase formed in response to local differentiation in cupolas, whilst the bulk of the Bethlehem and Bethsaida phases later crystallised within the main magma chamber.

The Witches Brook phase - which has been tentatively correlated with the Bethlehem phase by Northcote (1969) - exhibits the widest range of composition on Fig 13. A distinction has already been made (Chap. IV) between those samples containing only normally zoned plagioclase and those containing oscillatory zoned plagioclase, and this distinction is confirmed by Fig 13. The two samples containing oscillatory zoned plagioclases - a distinctive feature of the Bethlehem phase - have compositions that are essentially the same as those of the Bethlehem phase. The three samples with only normally zoned plagioclases

have compositions corresponding to those of the most highly differentiated LeRoy granodiorite. It is suggested therefore that the Witches Brook dyke-like phase of Northcote (1969) in fact represents two separate phases. The first of these is associated with the more differentiated late components of the early phases of the batholith, and the second is associated with the later, less differentiated Bethlehem phase. Both of these groups exhibit early euhedral plagioclase; later anhedral quartz and final anhedral, interstitial alkali feldspar.

The Spatsum quartz monzonite sample #31, which Northcote has tentatively equated with the Witches Brook phase, is the most highly differentiated sample studied. The rock contains roughly equidimensional subhedral quartz, plagioclase and alkali feldspar in the proportions 41:30:26 vol %, suggesting that crystallisation of these three minerals was almost simultaneous. The position of this sample on Fig 13 indicates that it lies very close to the hypothetical univariant curve.

During crystallisation of the Bethlehem phase a change in the order of formation of the felsic minerals occurred. Early (outer) Bethlehem phase samples contain large euhedral plagioclase crystals, some of which exhibit

a preferred orientation, set in a finer grained mosaic of plagioclase, quartz and alkali feldspar. This indicates early plagioclase crystallisation. The later (inner) Bethlehem phase and the Bethsaida phase contain large, subhedral, fractured quartz crystals which appear to be slightly resorbed phenocrysts. This is confirmed by the textural evidence exhibited by a dyke of Bethsaida granodiorite that cuts Guichon phase rocks east of the Bethlehem Copper property (White et al 1956). This dyke contains large euhedral to subhedral quartz phenocrysts set in a finer grained matrix of quartz and feldspar (see Photo 5). Thus it would appear that the later portions of the Bethlehem phase and the Bethsaida phase began crystallisation from within the quartz field of the 'granodiorite tetrahedron'. The essential similarity of the compositions of the Highland Valley phase and the Bethlehem/Bethsaida phases has already been noted. Thus progressive silica enrichment due to differentiation cannot be called upon to explain the presence of quartz phenocrysts in the later phases. Tuttle and Bowen (1958) and others have shown experimentally that progressive increases in PH_2O will cause progressive increases in the size of the quartz field in the system $\text{Ab-Or-Qz-H}_2\text{O}$. It is suggested therefore that the

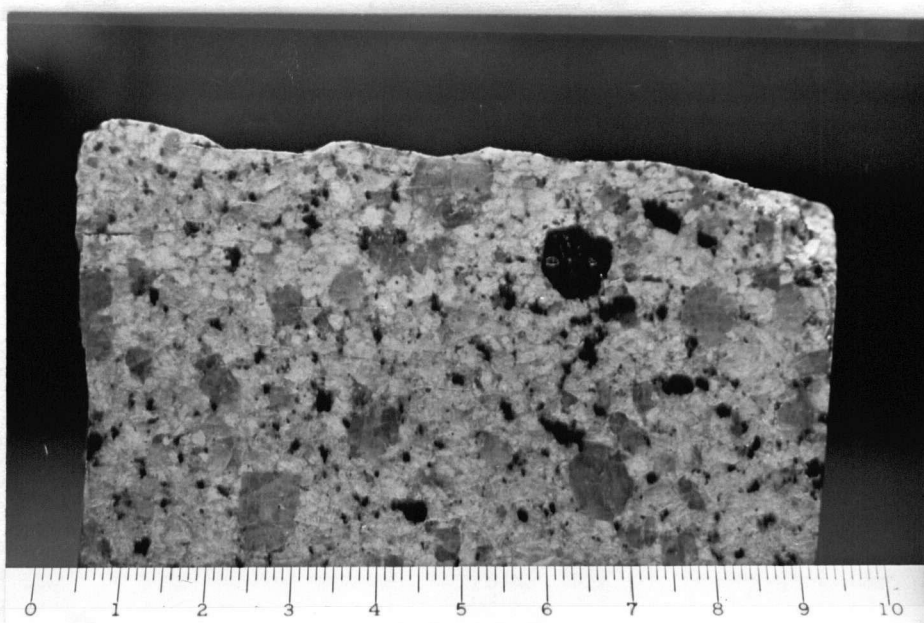


Plate 5 Sample from a chilled Bethsaida dyke from east of the Bethlehem Copper property. Note presence of subhedral-euhedral phenocrysts of quartz and euhedral poikilitic biotite. Scale in centimetres.

Bethlehem and Bethsaida samples containing early quartz phenocrysts may have crystallised under conditions of considerably higher volatile pressures than had previously existed. Experimental work in synthetic systems done by other investigators would seem to indicate that the presence of quartz on the liquidus in the 'granodiorite' system may require total pressures in the order of 4 or 5 kb (It must be emphasised however that this represents at best an 'inspired' estimate). Northcote (1969) has suggested that the Bethsaida phase crystallised in an epizonal environment, thus implying, at most, 6 to 8 km of cover which would produce a 'load' pressure in the order of 1.5 to 2 kb. If the above estimates are correct, it follows that the volatile pressures existing during crystallisation of the Bethsaida phase must have been in the order of 2 to 3.5 kb. Furthermore there is considerable evidence that conditions of high volatile pressures existed during the formation of many of the small, late igneous bodies that are believed related to the Bethlehem or/and Bethsaida phases. White et al (1956), for instance, explain the presence of numerous breccia pipes on the Bethlehem Copper property on the basis of subvolcanic explosions due to increasing volatile pressures.

Chemical estimates for the samples have been calculated

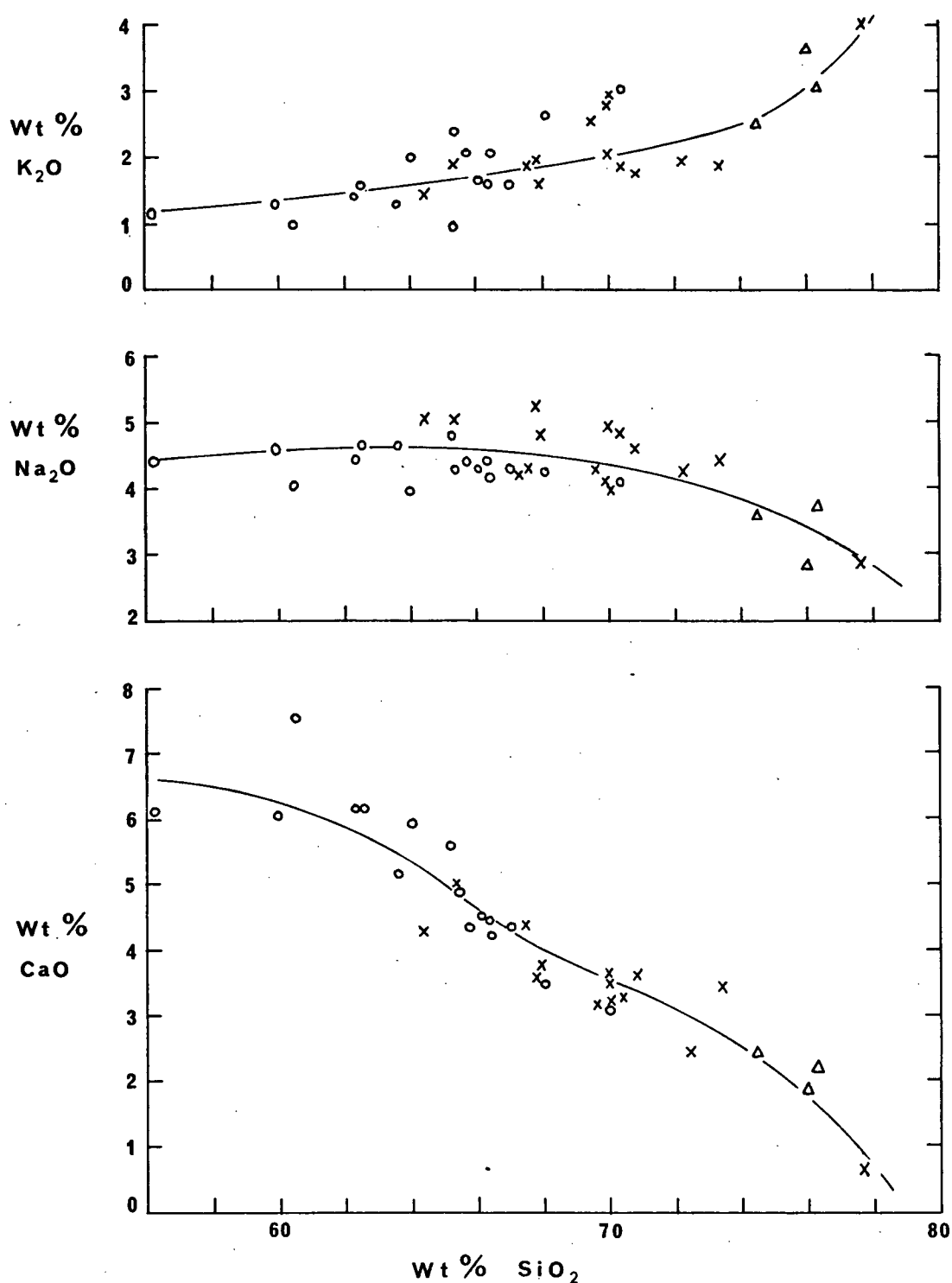


Fig. 14 Calculated component oxides as a function of silica content for the Guichon Creek batholith samples.

Hybrid and Highland Valley phases

Gump Lake phase

Bethlehem, Witches Brook and Bethsaida phases

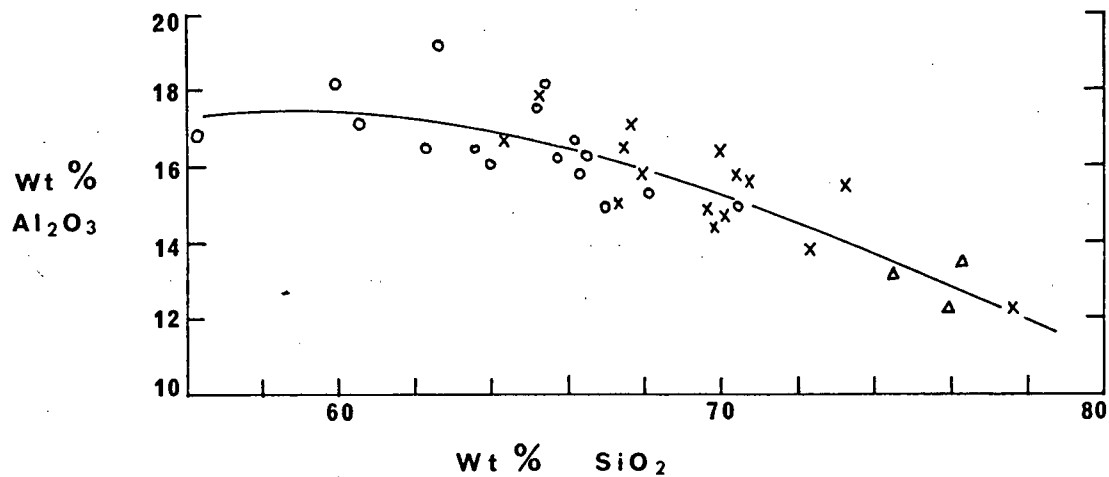
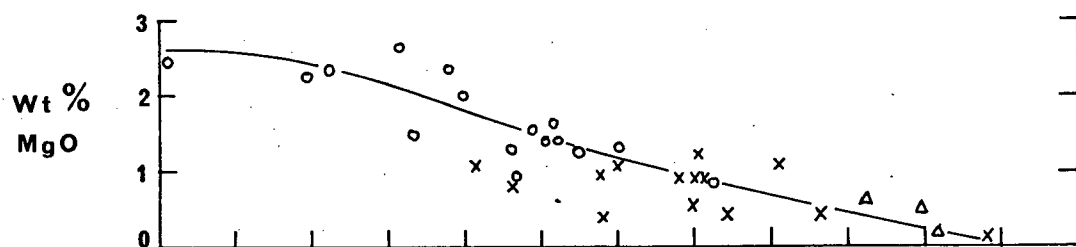
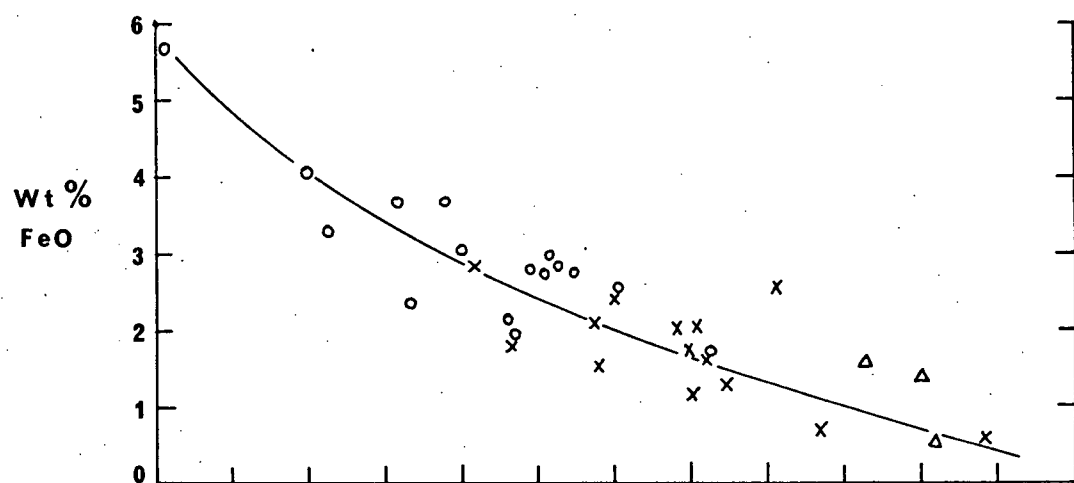
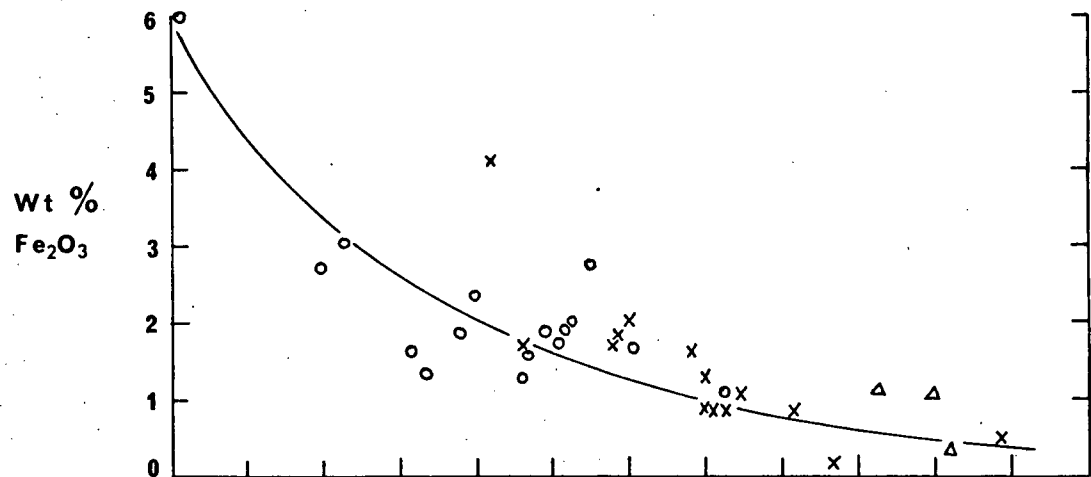


Fig. 14 continued

using the computer program of Dietrich and Sheehan (1964) modified for use on the University of British Columbia, I.B.M. 360 computer. The program assigns average chemical parameters to the minerals present in the mode and converts these to chemical estimates for the rock sample. Input is in the form of mineral volume percentages and output is presented as mineral weight percentages and component oxide weight percentages. Orthoclase, albite and anorthite are treated as separate mineral constituents, and therefore the data of Tables VI and VII was utilised for program input. Biotite, hornblende and augite analyses used were those from 'average' granodioritic rocks as reported in recent literature, and all opaque minerals were treated as magnetite. Chemical estimates are presented in Appendix 2 and silica variation diagrams for the component oxides are presented as Fig 14.

The diagrams emphasise the restricted range of compositional variation within the batholith, and also the overlapping nature of the compositional ranges of the various phases. The rather wide vertical scattering of data points on the variation diagrams is to be expected and is partly due to the errors inherent in modal analyses.

Fig 14 shows that the sequence Hybrid-Guichon-Chataway-LeRoy phases displays a progressive displacement

towards more silica rich compositions, which is probably largely the result of continuing differentiation. The later phases Bethlehem, Witches Brook and Bethsaida belong to the intermediate members of the series and very little discrimination can be made between them on the basis of the chemical estimates. The most acidic sample analysed comes from a small isolated body at the western margin of the batholith which Northcote has called the Spatsum Quartz Monzonite, and which he equates with the Witches Brook phase.

It has been suggested by Northcote that the Guichon phase approximates the composition of the original magma and that the more basic members of the pluton may be the result of assimilation of country rock during intrusion. The presence of a xenolith-rich zone extending for several hundred feet inwards from the outer margins of the Hybrid phase certainly tends to support this suggestion. An attempt has been made to construct an 'addition' diagram (c.f. Bowen 1928, p.76) to test the assimilation hypothesis. The average composition of the rocks intruded by the batholith is a particularly difficult parameter to estimate. The Permian Cache Creek Group adjacent to the present batholith contact is composed predominantly of andesitic greenstones with subordinate

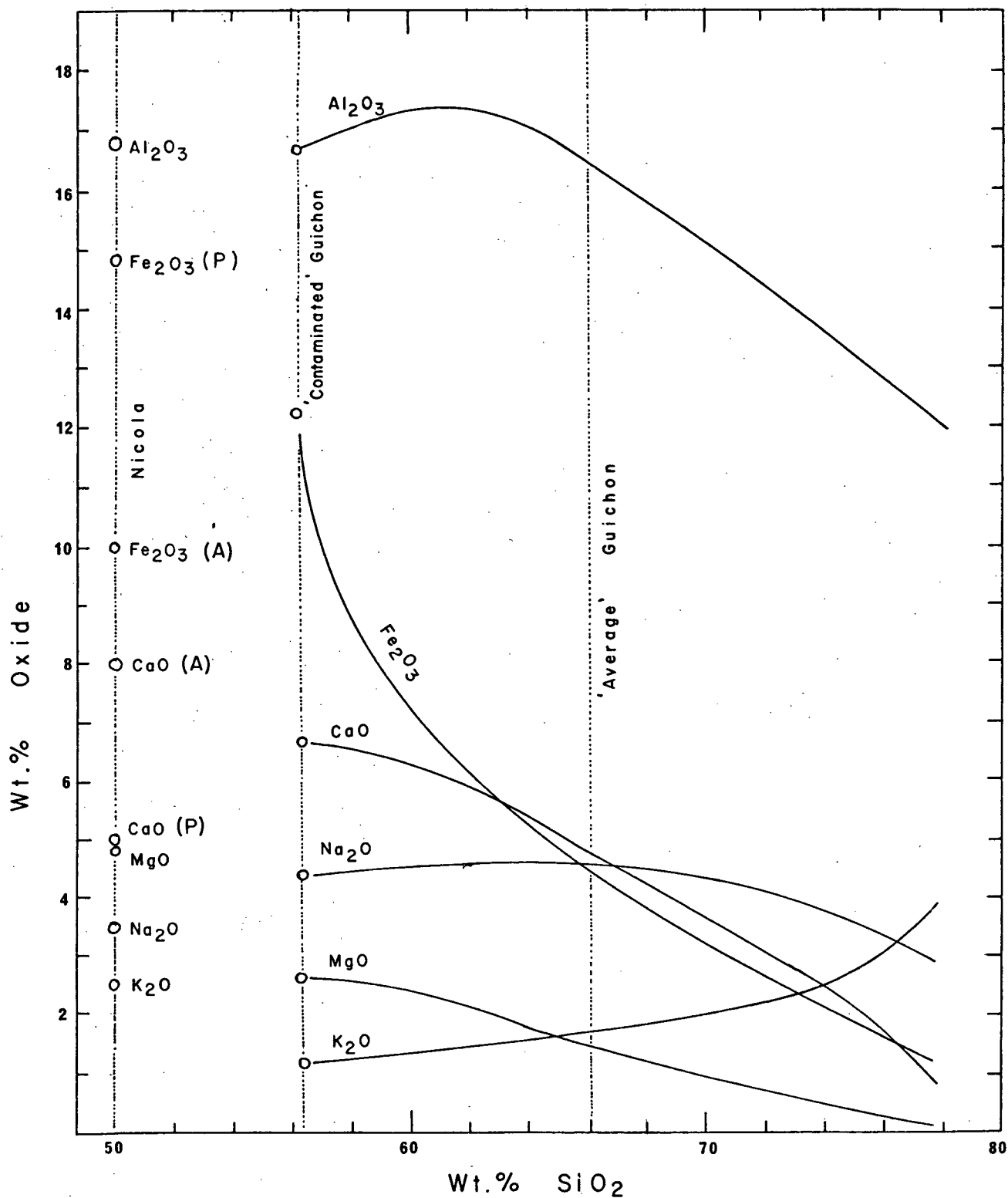


Fig. 15 Chemical compositions of proposed Guichon batholith primary magma ('average' Guichon), 'contaminated' Guichon rocks and Nicola Group extrusive rocks. Nicola analyses are from Schau (1968) and relate to his proposed 'A' and 'P' type extrusive cycles.

argillite and chert. The Upper Triassic Nicola group is predominantly andesitic or basaltic volcanic rocks with minor limestone, argillite, quartzite, greywacke and arkose. (Cockfield, 1947, Duffel and McTaggart, 1951). Schau (1969) has presented chemical analyses of volcanic rocks from the Nicola group. An average composition for the Nicola volcanic group taken from Schau's data, has been plotted on Fig 15 along with the established trends of chemical variation for the Guichon batholith samples. It is obvious that the 'average' Nicola volcanic, supposedly contaminated Guichon samples and the proposed Guichon magma compositions do not lie on straight line trends. The absence of such trends would tend to indicate that assimilation has not been a major factor in producing chemical variation through the batholith. It must be emphasised however that the variable amounts of sedimentary rock present in both the Nicola and Cache Creek groups may possibly have a significant effect on the composition of the assumed contaminating material. Bowen (1928) has emphasised that in order to melt basic material added to a more acidic magma considerable amounts of superheat would be necessary to prevent rapid crystallisation of the magma. The presence of preferentially oriented plagioclase crystals in

most of the Hybrid rocks suggests that the magma had reached liquidus conditions prior to intrusion and hence did not have any appreciable amount of superheat. Thus melting of any assimilated material is unlikely to have occurred. Bowen (1928) has suggested, however, that conversion of more basic material into constituents that are in equilibrium with the acid magma may take place without melting. Northcote (1969) has reported xenoliths within the Hybrid phase which display a marked variation in degree of assimilation. Some xenoliths have sharp angular outlines whilst others are reduced to indistinct clusters of mafic minerals. This suggests that the more acidic components of the xenoliths may have been more easily converted into constituents in equilibrium with the magma than the more basic components. If such is the case it would explain the lack of agreement between the evidence from the field and that from the 'addition' diagram of Fig 15.

An alternative hypothesis for the origin of the more basic rocks is that they are the direct result of magmatic differentiation. The foliated nature of the early phases of the batholith suggests that magmatic flow has occurred, possibly as a result of natural convection within the magma chamber. If convective flow did take place during

intrusion there exists the possibility that early formed crystals - predominantly oligoclase and pyroxene - may become attached to the roof or walls of the magma chamber, thus successively enriching the magma in more acidic components. In all probability magmatic differentiation and subordinate assimilative action have combined to produce the range of compositions exhibited by the earlier phases of the batholith.

The return to the chemically intermediate members of the series exhibited by the Bethlehem and Bethsaida phases, when combined with the evidence of plagioclase zonation schemes - as discussed on page 34 - suggests that a renewed intrusion of the magma occurred prior to consolidation of the Bethlehem phase. Textural information suggests that the bulk of this magma crystallised under fairly quiescent conditions. It seems likely, therefore, that the range of chemical compositions exhibited by these phases is largely the result of local heterogeneities caused by incomplete mixing of magma. The compositional ranges may also be partly due to errors in the modal analyses from which chemical estimates were calculated.

VII Geological Evolution of the Batholith

The history of emplacement of the Guichon Creek batholith has previously been discussed by Northcote (1969) and the following interpretation is largely an extension of Northcote's ideas. The only significant difference between the two schemes is that the present work suggests that convective magma flow has been largely responsible for the textural and compositional difference between successive phases. The possibilities of magma convection have been discussed by Grout (1918), Knopoff (1964), Shaw (1965) and Bartlett (1969), and these authors have concluded that convection may constitute a significant physical factor during the crystallisation of granitic magmas. Shaw (1965) also suggests that pockets of strongly differentiated liquid may develop close to the top of a magma chamber due to the action of local high level convective vortices.

Very little is known concerning the ultimate origin of the magma that crystallised to form the Guichon Creek batholith. Christmas et al (1969) have investigated the strontium isotopic composition of rocks from the batholith and from the Craigmont mine. They report an initial $\text{Sr}^{87}/\text{Sr}^{86}$ ratio for the Craigmont isochron of 0.7037 which falls within the range of values from recent

basalts (0.703-0.706). They conclude therefore "... that the ore minerals and K-feldspar gangue did not originate by fusion of ancient sialic basement or Cache Creek or Nicola rocks, but must have developed in an environment with low $\text{Sr}^{87}/\text{Sr}^{86}$ ratios similar to recent basalt. Such a source could be either reabsorbed oceanic crust (Wilson 1968), the upper mantle or a basic layer in the lower part of the crust....". They further imply that the magma which formed the Guichon batholith developed in a similar environment. Initial rise of early magma was possibly due to gravitational instability of the less dense magma in relation to the rocks present at the place of formation. Intrusion of the early granitic magma was probably controlled by the dominantly NW-SE strike of the country rocks and may have been in part accomplished by magmatic stopping, as evidenced by the xenoliths present in the outer phases of the batholith.

Although the temperature of the early magma at the time of emplacement need not have been very high, the temperature difference between magma and country rock would probably have been considerable. In such cases conduction of heat into the wallrocks at the margin of the intrusion may well have led to a temperature differential within the chamber which could not be

satisfied by conduction of thermal energy through the magma. This in turn would precipitate magma convection. A combination of intrusive flow and magmatic convection would account for the foliation of plagioclase crystals observed in the outer phases of the batholith. Relative movement of magma and crystallising plagioclase, as might be expected to occur during magmatic convection, would also explain the normal zoning exhibited by plagioclases from Hybrid and Highland Valley phases. Possible concentration of early formed mineral phases - primarily plagioclase and pyroxene - at the periphery of the magma chamber, combined with local assimilation of country rock and a progressive inwards solidification, probably led to a gradual enrichment of the remaining magma in acidic components. In this manner the observed gradual change in rock composition during crystallisation of the Hybrid and Highland Valley phases may have been accomplished.

The observed foliation of both plagioclase and mafic minerals in a large part of the Guichon Variety, in addition to its intrusive nature into the Hybrid phase, suggested to Northcote that a magmatic pulse must have occurred during crystallisation of the Highland Valley phase. This intrusive movement must have occurred when

crystallisation of the Guichon variety was fairly well advanced, and movement would have taken the form of flowage of a largely crystalline mush. The conditions of crystallisation of the Chataway variety must have been very similar to those existing during crystallisation of the Hybrid phase. The only observable differences between these two units are that the Chataway variety crystallised from a more acidic magma and that assimilation was largely inoperative. The continuing trend of differentiation is exhibited by the LeRoy granodiorite phase. The dyke like nature of this phase has been ascribed by Northcote to local increases in volatile pressures possibly within cupolas at the roof of the magma chamber, which exceeded confining pressure and strength of overlying rock, causing fracturing in cooler crystalline phases.

The Gump Lake phase does not appear to be directly related to the other phases of the Guichon batholith. As explained in Chapter VI, it is suggested that the Gump Lake phase may be an offshoot of the Nicola Batholith which outcrops to the east. Because of the relatively small size of the Gump Lake phase, and its intrusion into rocks already heated by previous phases, it is probable that conductive heat transfer through the

magma was able to keep pace with relatively slow heat loss to the surrounding rocks and hence magma convection never developed. Such conditions would explain the lack of foliation and the coarse-grained, equigranular nature of this phase. Textural evidence suggests that plagioclase and quartz crystallised essentially simultaneously from the Gump Lake magma.

The return to more intermediate bulk compositions and the complete change in the nature of plagioclase zoning schemes exhibited by the Bethlehem and Bethsaida phases indicate a renewed influx of magma into the area. The composition of this magma was more basic than that which crystallised the LeRoy granodiorite and yet more acidic than the bulk composition of the earlier magma. The emplacement of the later magma was probably governed largely by zones of weakness originally created by the earlier magma, and the processes involved are believed to have included at least minor remelting of Highland Valley phase rocks. Remelting is suggested by plagioclase zoning schemes (discussed earlier, p. 41) in Witches Brook phase rocks, which Northcote believes to be an associated dyke phase of the Bethlehem phase. In view of the close compositional similarity between Highland Valley and

Bethlehem phase rocks the problems of assimilation seem not to be insurmountable.

The intrusion of the later magma into batholithic rocks that were probably already at elevated temperatures may have precluded the formation of any significant temperature gradient, and hence magmatic convection, in all probability, did not occur. If the presence of delicate oscillatory zoning in plagioclase feldspars is due to the process expounded by the diffusion-supersaturation theory of Harloff (1927) and later workers, then the crystallisation of the Bethlehem and later phases must have taken place under very quiescent conditions. An apparent contradiction to this, however, is the presence of an imperfect plagioclase preferred orientation in the outer parts of the Bethlehem phase. Local convection and/or intrusive flow may have occurred at the periphery of the magma chamber during early crystallisation causing orientation of plagioclase crystals. If such flow occurred during early stages of plagioclase crystallisation it is just conceivable that the viscosity of the magma prevented relative crystal-liquid boundary layer movement and oscillatory zoning continued uninterrupted. During consolidation of the Bethlehem phase the volatile pressures within the magma chamber must have risen

considerably thus permitting the initial crystallisation of quartz rather than plagioclase.

On the basis of textural and field evidence, Northcote (1969) has suggested that the early phases of the batholith were emplaced under mesozonal conditions, and that progressive erosion of the cover rocks established epizonal conditions before emplacement of the later phases. The possibility exists that a relatively long time interval separated the emplacement of early and late phases of the batholith. The nature of the contacts between Bethlehem and Highland Valley phases - which vary from sharply intrusive to gradational - suggests to the present author, however, that the two phases were separated by a relatively short time interval. Northcote also has suggested that the emplacement and crystallisation of the early phases may have occupied only four million years. The present author has argued that the intrusion of the later magma into rocks that were probably already at elevated temperatures prevented convective flow and hence the later phases crystallised under essentially quiescent conditions in the presence of high volatile pressures. Thus the change in textural features from early to late phases may possibly be explained by variation in physical parameters other than those

controlled by depth of intrusion. The mineralogical variations presented in the present thesis contain no evidence to support any great changes in depth occurring during crystallisation of the main phases of the batholith. The presence of local breccia pipes, within the Guichon batholith, certainly suggests that the very late stage igneous activity took place under epizonal type conditions.

Is it possible that the entire batholith crystallised under epizonal conditions? Northcote has listed criteria present within the older phases of the batholith which - according to Buddington (1959) - would suggest mesozonal crystallisation (see Table X). The presence of all these features within an epizonal environment could be adequately explained if convection was active within the magma chamber, thus causing a continuing, relatively rapid transfer of heat to the chamber margins. This could account for the presence of complex emplacement relationships to country rock, contact metamorphism of epidote-amphibolite grade and partial assimilation of country rock. The presence of preferentially oriented plagioclase crystals within the older phases of the batholith may be evidence that convection was occurring during their crystallisation. If such is the case then the apparent change from mesozonal to epizonal conditions

TABLE X Criteria, suggested by Buddington (1959) as indicative of mesozonal intrusion, which are present in the Guichon Creek batholith
(From Northcote, 1968)

- a) Degree of metamorphism of country rocks not more intense than green-schist and epidote-amphibolite facies (400-500°).
- b) Complex emplacement relationships to country rock; in part discordant, in part concordant. Local replacement.
- c) Planar foliation is often well developed, especially in outer portions of the pluton, but is commonly local, elusive or missing in the core.
- d) Younger units may cross cut foliation of older units, or the structure may locally be independent of boundary units within a composite pluton.
- e) Assimilation may be significant in border or roof zones.
- f) Emplacement by reconstitution and replacement is commonly absent or subordinate.
- ? g) Chill border facies, in the sense of aphanitic texture, are absent. (Present in the youngest phases of the Guichon batholith).
- h) Migmatites are absent or subordinate.
- i) Pegmatites and aplites common especially in the border zones. They may have a radial fabric.
- j) Mirolitic structure is absent.
- k) Contact metamorphic aureoles may be well developed.

suggested by Northcote may not be real and the erosion of several thousands of feet of Lower Jurassic sediments during the emplacement of the batholith may not be necessary. The present author would suggest therefore that during crystallisation of the batholith the level of emplacement of the batholith, i.e. the depth of cover, may have changed by as little as two kilometres.

It has already been stated that crystallisation of the bulk of the Bethlehem and Bothsaida phases is believed to have occurred under essentially quiescent conditions. The slow cooling of the magma under such conditions naturally led to the crystallisation of the coarse grained, even textured Bothsaida phase. Textural evidence suggests that the Bothsaida phase crystallised under conditions of high volatile pressures. The continuing enrichment of the magma in volatiles and consequent increases in volatile pressures probably eventually resulted in local fracturing of the walls of the magma chamber. Local fracturing was accompanied by emplacement of porphyry dyke swarms, pipe breccias and possibly the Gnawed Mountain Porphyries. Local emplacement of Bothsaida phase dykes into older phases also occurred at this time. Copper-rich mineral deposits such as Bethlehem, Trojan, Krain, O.K. and Lornox accompanied this final igneous activity.

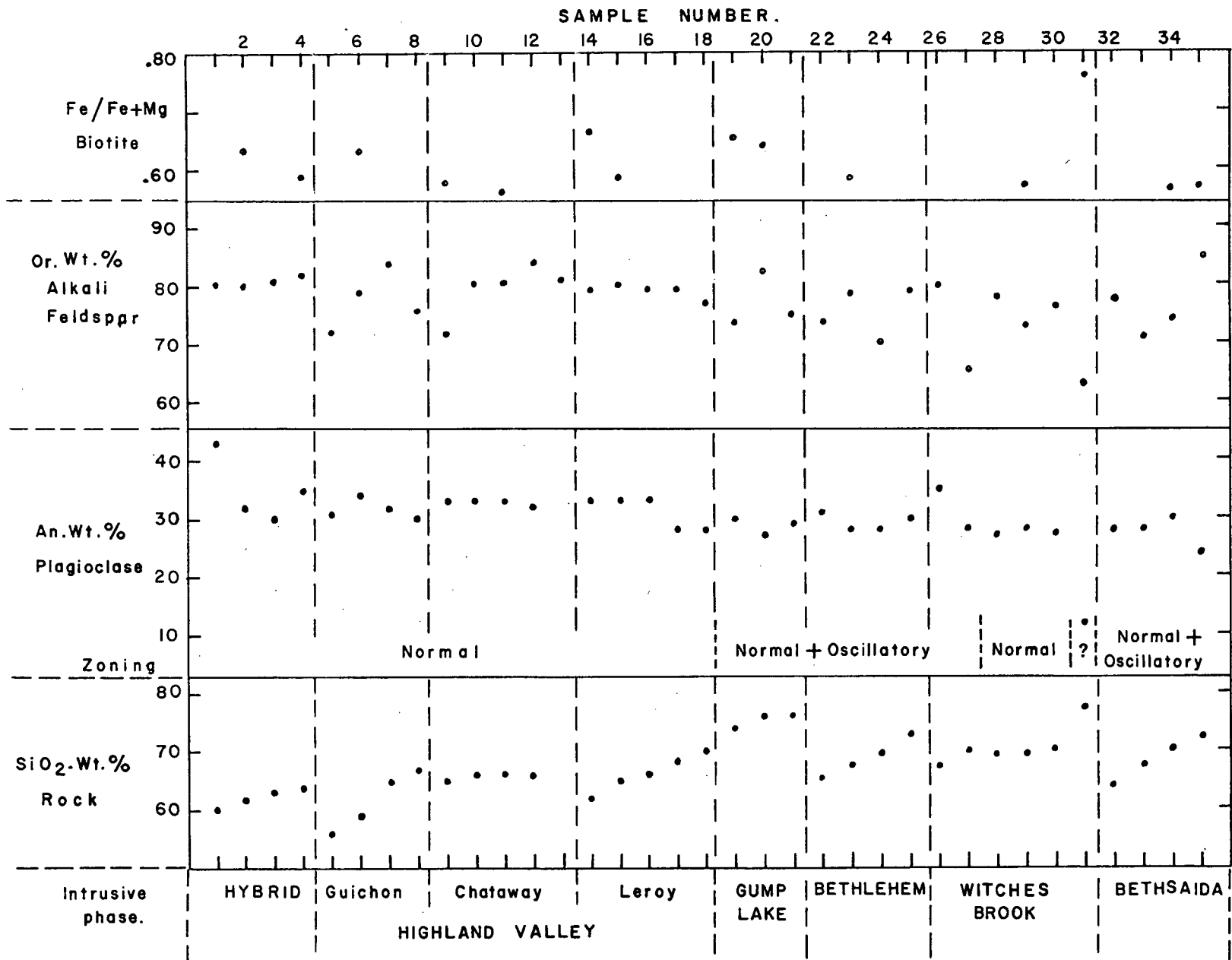


Fig 16: Summary of compositional variations in the Guichon Creek batholith.

VIII Summary and Conclusions

The present study has been concerned with the changing mineralogical composition of the rocks produced during crystallisation of the Guichon Creek batholith. The study has shown that, in general, there was a slow progressive change in the relative proportions of various mineral phases present in the rocks as crystallisation of the batholith proceeded. The chemical compositions of the individual mineral phases, however, show very little change with decreasing relative age of the host rock. (Fig 16).

Alkali feldspars throughout the batholith are microperthitic and the potassium rich phases of these have structural states equivalent to that of orthoclase. The two unmixed phases of the alkali feldspar are almost pure orthoclase and pure albite respectively. The bulk compositions of artificially homogenised alkali feldspars from the batholith range from 71 to 86 Wt% Or. There is a seemingly random variation of bulk compositions and structural states of the alkali feldspars from the various phases of the batholith.

Plagioclase feldspars from the batholith are of low or intermediate structural states. Plagioclase from the Hybrid and Highland Valley phases show normal zoning with

cores An_{48-32} and rims An_{28-20} . The Gump Lake phase carries oscillatory zoned plagioclases with cores An_{32} and rims An_{20} . Plagioclases from the Bethlehem and Bethsaida phases exhibit oscillatory zoning with cores An_{38-28} and rims An_{20} . The Witches Brook phase may contain plagioclases similar to those of either the Highland Valley or the Bethlehem phase. In many of the samples studied partial resorption of plagioclase occurs at plagioclase-alkali feldspar grain boundaries.

There is an approximate correlation between the silica content of any rock and the concentration of biotite that it contains. Within the major phases of the batholith there is also a slight regular decrease in the $Fe/Fe + Mg$ ratio of the biotite with increasing silica content of the host rock in which it is found. The $Fe/Fe + Mg$ ratio in biotites also appears to be affected by the presence of any other ferromagnesian silicates. Thus in those rocks containing more than 73 Wt% SiO_2 biotite is the only ferromagnesian silicate present, and the $Fe/Fe + Mg$ ratios in these biotites increases rapidly with further increases in the silica content of the host rocks. Such conditions are found only in the samples from the Gump Lake phase - which may not be genetically related to the rest of the Guichon Creek

batholith - and from the Spatsum quartz-monzonite which is believed to be a late stage differentiate of the batholith. The variations in $\text{Fe}/\text{Fe} + \text{Mg}$ ratios in biotites may be produced by variable fugacities of oxygen which in turn may be controlled by the presence or absence of other ferromagnesian silicate phases.

The variable textures and compositions present in the Guichon Creek batholith are the products of crystallisation of magma under varying physical conditions. These conditions included assimilative reaction with country rocks, magmatic convection and differentiation and varying volatile and oxygen pressures. Two distinctive events in the crystallisation history can be discerned from the mineralogical study. The first major event produced the Hybrid, Highland Valley and LeRoy phases of the batholith, the second major event produced the Bethlehem, Witches Brook and Bethsaida phases and the minor late stage porphyrys and breccias associated with them. The Gump Lake phase was intruded at some time between the two major events outlined above but its genetic relationship to the rest of the batholith is in doubt. It appears from analysis of modal salic constituents that the Gump Lake phase is not directly related to the other phases of the Guichon batholith and it may possibly be genetically linked to the Nicola batholith which outcrops

to the east.

There is a definite chemical and mineralogical change in the nature of the batholithic rocks with decreasing relative age of intrusion. The early magmatic event was probably accompanied by at least minor assimilative action and convective flow of the magma. These conditions produced the xenolith rich margin to the batholith, the preferred orientation of normal zoned plagioclase phenocrysts in the early phases and progressively less basic bulk compositions through the Hybrid and Highland Valley phases. The LeRoy granodiorite was emplaced as a dyke phase possibly as a result of locally high volatile pressures existing in cupolas at the batholith margin. The more highly differentiated nature of the LeRoy granodiorite is compatible with such an origin. The sequence of crystallisation of the salic mineral phases during the early magmatic event was: plagioclase, quartz, alkali feldspar; and the mafic mineral phases crystallised in the sequence: pyroxene (not common), hornblende, biotite. The presence of pyroxene inclusions in plagioclase cores suggests that pyroxene was the first major mineral phase to separate in pyroxene bearing rocks. The lack of mafic inclusions in plagioclase cores in rocks devoid of pyroxene suggests that hornblende and biotite crystallised after the first separation of plagioclase in

these rocks.

The later magmatic event is most probably directly, genetically related to the earlier magmatic event and records a slight renewed intrusive movement. This magma crystallised under quiescent conditions and thus very little differentiation took place. The lack of convective flow in this magma was probably due to its emplacement into hot, consolidated rocks of the earlier event and for this reason also the later magma crystallised to a much coarser grain size. The conditions of emplacement of the Witches Brook phase were very similar to those of the LeRoy granodiorite of the early magmatic event. Plagioclase zoning schemes and bulk composition data suggest that some samples originally described by Northcote (1969) as belonging to the Witches Brook phase may in fact belong to the LeRoy granodiorite phase. During crystallisation of the later magma a change in the order of crystallisation of the silic mineral phases occurred. Thus initial separation of plagioclase in the outer Bethlehem phase was replaced by initial separation of quartz in the Bethsaida phase. This change was most probably due to an increase in the volatile pressures. If results from synthetic experimental investigations can be directly applied to the present case it suggests

that total pressures in the order of 4 kilobars existed during crystallisation of the Bothsaida phase. The observed gradual decrease in $\text{Fe}/(\text{Fe} + \text{Mg})$ ratios in biotites in rocks of both the earlier and later magmatic events suggests that the fugacity of oxygen was also increasing gradually during consolidation of the major phases of the batholith. The continued build up of volatile pressures within the magma chamber eventually led to local fracturing of the chamber margins and the formation of prophyry dykes, pipe breccias and local economic mineral deposits.

Northcote (1969) has suggested that a change from mesozonal to epizonal emplacement environments occurred during consolidation of the batholith. Due to the lack of any evidence to suggest that successive phases penetrated en masse into successively higher regions of the crust Northcote has suggested that from 5000 ft to 15000 ft of Lower Jurassic sediments were eroded from the roof of the batholith during its emplacement. The mineralogical data collected in the present thesis contains no evidence to support any great changes in depth occurring during crystallisation of the main phases of the batholith. The present author would suggest therefore that the physical characteristics of the

batholith that suggest mesozonal emplacement may perhaps be due to a combination of epizonal emplacement and the action of convection within the magma chamber. If such is the case the depth of emplacement may have changed by as little as 2 km during the entire crystallisation history of the batholith.

REFERENCES CITED

- Alling, H.L.; 1938: Plutonic perthites: Jour. Geol., v.46, p.142.
- Baadsgard, H., Folinsbee, R.E. and Lipson, J. 1961: Potassium-Argon dates of Biotites from Cordilleran Granites: Geol. Soc. Am., Bull., v.72, pp. 689-702.
- Bartlett, R.W.; 1969: Magma Convection, Temperature Distribution and Differentiation: Am. Jour. Sci., v.267, pp. 1067-1082.
- Bottinga, Y.; Kudo, A., and Weill, D., 1966: Some observations on oscillatory zoning and crystallisation of magmatic plagioclases: Amer. Min, v.51, pp. 792-806.
- Bowen, N.L.; 1928: The evolution of the igneous rocks: Dover Pub. Inc.
- Brown, B.E.; 1962: Aluminum distribution in an igneous maximum microcline and the sanidine microcline series: Norsk. Geol. Tidsskr., v.42, pp. 25-36.
- Buddington, A.F.; 1959: Granite emplacement with special reference to North America: Bull. Geol. Soc. Am., v.70, pp. 671-747.
- Carr, J.M.; 1960: Porphyries, breccias, and copper mineralisation in the Highland Valley, B.C.: Can. Min. Jour., v.81, pp. 71-73.
- ; 1961 : Geology of the promotory hills: Minister of Mines and Pet. Res., B.C., Ann. Rept., 1960, pp. 26-40.
- ; 1963: The geology of part of the Thompson River valley between Ashcroft and Spences Bridge: Minister of Mines and Pet. Res., B.C., Ann. Rept., 1962, pp. 28-45.
- Christmas, L.; Baadsgard, H.; Folinsbee, R.E.; Fritz, P., Krouse, H.R. and Sasaki, A., 1969: Rb/Sr, S, and O isotopic analyses indicating source and date of contact metasomatic copper deposits, Craigmont, British Columbia, Canada: Econ. Geol. v.64, pp. 479-488.

- Cockfield, W.E.; 1948: Geology and mineral deposits of Nicola map area, British Columbia: Geol. Surv. Canada, Mem. 249.
- Dietrich, R.V.; and Sheehan, D.M., 1964: Approximate chemical analyses from modal analyses of rocks: Virginia Polytechnical Inst., Extension Series Circular 1.
- Dirom, G.E.; 1965: Potassium - argon age determinations on biotites and amphiboles, Bethlehem copper property, B.C.: M.A.Sc. thesis, Univ. of British Columbia (unpublished)
- Duffell, S.; and McTaggart, K.C.; 1952: Ashcroft map area, British Columbia: Geol. Surv. Canada, Mem. 262.
- Evans, H.T.; Appleman, D.E.; and Handwerker, D.S.; 1963: The least squares refinement of crystal unit cells with powder diffraction data by an automatic computer indexing method (abs.): Program, Annual Meeting, Am. Cryst. Assoc., March 1963, Cambridge Mass., pp. 42-43.
- Franco, R.R., and Schairer, J.F.; 1951: Liquidus temperatures in mixtures of the feldspars of soda, potash and lime: J. Geol., v. 59, pp. 259-267.
- Gower, J.A.; 1957: X-ray measurement of the iron magnesium ratio in biotites: Am. Jour. Sci, v.225, pp. 142-156.
- Harloff, C.; 1927: Zonal structures in plagioclase: Leidsche Geol. Mededeel. v.2, pp. 99-114.
- Haslam, W.H.; 1968: The crystallisation of intermediate and acid magmas at Ben Nevis, Scotland: Jour. Pet., v. 9, pp. 84-104.
- Hills, E.S.; 1936: Reverse and oscillatory zoning in plagioclase feldspars: Geol. Mag., v.73, pp. 49-56.
- James, R.S.; and Hamilton, D.L., 1969: Phase relations in the system $\text{NaAlSi}_3\text{O}_8$ - KAlSi_3O_8 - SiO_2 at 1 kilobar water vapour pressure: Contr. Mineral. and Petrol., v.21, pp. 111-141.

- Knopoff, L.; 1964: The convection current hypothesis: Rev. Geophysics, v.2, pp. 89-123.
- Laves, F., and Goldsmith, J.R.; 1961: Polymorphism, order, disorder, diffusion and confusion in the feldspars: Inst. "Lucas Mallada", Cursillos Conf., v. 8, pp. 71-80.
- Luth, W.C., Jahns, R.H., and Tuttle, O.F.; 1964: The granite system at 4 to 10 kilobars: J. Geophys. Research, v. 64, pp. 759-773.
- Northcote, K.E.; 1968: Geology and geochronology of the Guichon Creek Batholith, B.C.: PhD. Thesis, Univ. of British Columbia. (unpublished)
- ; 1969: Geology and geochronology of the Guichon Creek Batholith: B.C. Dept. of Mines and Pet. Res., Bull. 56.
- Orville, P.M.; 1967: Unit cell parameters of the microcline - low albite and the sanidine - high albite solid solution series. Am. Miner., v. 52, pp. 55-86.
- Piwinski, A.J.; 1968: Experimental studies of igneous rock series, central Sierra Nevada batholith, California: Journ. Geol. v.76, pp. 548-570.
- ; and Wyllie; P.J., 1968: Experimental studies of igneous rock series: A zoned pluton in the Wallowa batholith, Oregon: Ibid. v.76, pp. 205-234.
- Platen, H.V.; 1965: Experimental anatexis and genesis of migmatites. In: Controls of metamorphism, ed. by W.S. Pitcher and G.W. Flinn, Oliver and Boyd.
- Rimsaite, J.H.Y.; 1967: Studies of rock-forming micas: Geol. Surv. Canada, Bull. 149.
- Schairer, J.F., and Bowen, N.L.; 1947: System $\text{CaAl}_2\text{Si}_2\text{O}_8$ - SiO_2 . Bull. soc. geol. Finland, v. 20, p. 71.
- Schau, M.P.; 1968: Geology of the Upper Triassic Nicola Group in south-central British Columbia: PhD. Thesis, Univ. of British Columbia (unpublished)

- Shaw, H.R.; 1965: Comments on viscosity, crystal settling and convection in granite magmas: *Am. Jour. Sci.*, v. 263, pp. 120-152.
- Smith, J.V.; 1956: The powder patterns and lattice parameters of plagioclase feldspars. I. The sodium rich plagioclases: *Mineral. Mag.*, v. 31, pp. 47-68.
- ; and MacKenzie, W.S.; 1961: Atomic, chemical and physical factors that control the stability of alkali feldspars: *Inst. "Lucas Mallada", Cursillos Conf.*, v. 8, p. 39.
- Stewart, D.B.; 1967: Four phase curve in the system $\text{CaAl}_2\text{Si}_2\text{O}_8 - \text{SiO}_2 - \text{H}_2\text{O}$ between 1 and 10 kilobars: *Schweiz. mineral. petrogr. Mitt.*, v.47, pp. 35-59.
- ; and Ribbe, P.H.; 1969: Structural explanation for variations in cell parameters of alkali feldspar with Al/Si ordering: *Am. Jour. Sci.*, Schairer Vol. 267-A, pp. 444-562.
- Tilling, R.I.; 1968: Zonal distribution of variations in the structural state of alkali feldspar within the Rader Creek pluton, Boulder batholith, Montana: *Jour. Pet.*, v.9, pp. 331-357.
- Tuttle, O.F., and Bowen, N.L.; 1958: Origin of granite in the light of experimental studies in the system $\text{NaAlSi}_3\text{O}_8 - \text{KAlSi}_3\text{O}_8 - \text{SiO}_2 - \text{H}_2\text{O}$: *Geol. Soc. Amer. Mem.* 74.
- Vance, J.A.; 1962: Zoning in igneous plagioclase: normal and oscillatory zoning: *Am. Jour. Sci.*, v. 260, pp. 746-760.
- Wanless, R.K., Stevens, R.D., Lachance, G.R., and Rimsaite, J.H.Y.; 1965: Age determinations and geological studies: *Geol. Surv. Canada Paper* 64-17, Pt.1.
- Wanless, R.K., Stevens, R.D., Lachance, G.R., and Edmonds, C.M.; 1967: Age determinations and geological studies: *Geol. Survey Canada. Paper* 67-2. Pt.A. pp. 35-39.

- White, W.H., Thompson, R.M., and McTaggart, K.C.; 1957: The geology and mineral deposits of the Highland Valley, British Columbia: C.I.M.M. Trans., vol. 60, pp. 273-289.
- White, W.H., Erickson, G.P., Northcote, K.E., Dirom, G.E., and Harakal, J.E.; 1967: Isotopic dating of the Guichon batholith, B.C.: Can. Jour. Earth Sci., v.4, pp. 677-690.
- Wilson, J.T.; 1968: A revolution in earth science: C.I.M. Bull., v.61, No.670, pp. 185-192.
- Wones, D.R., and Eugster, H.P.; 1965: Stability of biotite: experiment, theory and application: Am. Miner. v.50, pp. 1228-1272.
- Wright, T.L.; 1968: X-ray and optical study of alkali feldspar II. An X-ray method for determining the composition and structural state from measurement of 20 values for three reflections: Am. Miner., v.53, pp. 88-104.
- ; and Stewart, D.B.; 1968: X-ray and optical study of alkali feldspar. I. Determination of composition and structural state from refined unit cell parameters and 2v: Ibid., v. 53, pp. 38-87.
- Yoder, H.S., Jr., Stewart, D.B., and Smith, J.R.; 1957: Ternary feldspars: Yb. Carnegie Instn. Wash. v.56, pp. 206-214.
- Yoder, H.S. Jr.; 1967: System Ab-An-Q-H₂O at 5 kb: Ibid, v.66, pp. 477-478.

Appendix 1 Petrographic Descriptions

The following petrographic descriptions are concerned primarily with textural features present in the samples. For modal analyses see Appendix 2. Sample numbers given in brackets relate to the original field sample number used by K.E. Northcote who collected all the samples used in this study. Grain sizes are given in terms of the greatest dimension.

HYBRID PHASE

1. (K64-59A) Quartz Diorite

Medium grained, equigranular, marked preferred orientation of plagioclase. Plagioclase subhedral-euhedral, wide range in grain size from 2.5mm - 0.5mm., very weak normal zoning, strong sericitic alteration. Orthoclase perthitic, interstitial or poikilitically enclosing all other minerals. Quartz anhedral, interstitial. Mafics are ragged, anhedral and relatively fresh. Clinopyroxene is subhedral and of approx. 1 mm grain size. Hornblendes have cores of strongly altered clinopyroxene and contain inclusions of plagioclase, magnetite and quartz. Biotite is partly poikilitic, enclosing hornblende, quartz, plagioclase and opaques. Myrmekite present at some plagioclase - orthoclase grain boundaries, if absent plagioclase has albitic rim and is partially resorbed.

2. (K64-49A) Quartz Diorite

Very similar to sample #1 except for presence of traces of microcline twinning in the alkali feldspar. Clinopyroxene occurs only as cores to hornblende.

3. (K64-13) Quartz Diorite

Very similar to sample #1 except that clinopyroxene occurs only as cores to hornblende.

4. (k64-156A) Granodiorite

Fine-medium grained, equigranular, marked preferred orientation of plagioclase. Plagioclase subhedral, grain size 2mm, fresh, normal zoning. Quartz anhedral, interstitial. Orthoclase interstitial, very few plagioclase inclusions (strongly resorbed), some myrmekitic

intergrowths. Clinopyroxene ragged, subhedral with plagioclase inclusions. Biotite markedly interstitial poikilitic forming grains with max. size 3mm.

HIGHLAND VALLEY PHASE

Guichon Variety

5. (K63-196-I) Contaminated ? Quartz Diorite

Medium-coarse grained granular texture, marked plagioclase preferred orientation, mafic minerals tend to form clusters. Plagioclase subhedral-euhedral, normal zoning, marked alteration. Quartz and orthoclase interstitial. All mafics extremely ragged. Clinopyroxene rimmed by hornblende and variably replaced by sieve texture hornblende. Biotite poikilitic enclosing plagioclase, quartz, mafics and sphene, extensive alteration to chlorite.

6. (K63-71A) Quartz Diorite

Medium grained, equigranular, preferred orientation of larger plagioclase crystals. Plagioclase is subhedral-euhedral, exhibits weak normal zoning, considerable sericitic alteration and partial resorption where it is in contact with alkali feldspar. Plagioclase grain size ranges from 3mm to .5mm. Quartz is interstitial to plagioclase, anhedral and exhibits strong extinction mosaics. Orthoclase is anhedral, poikilitic or interstitial enclosing plagioclase and hornblende. Hornblende is ragged but subhedral, often has cores of clinopyroxene and tends to form clusters of grains. Biotite is ragged and generally anhedral with strong chloritic alteration and quartz stringers are present along the cleavage. Biotite generally about 1mm but may be poikilitic up to 3mm. Opaque minerals show a strong association with biotite and hornblende.

7. (K63-104-I) Granodiorite

Medium-coarse grained equigranular. Plagioclase euhedral-subhedral, 4mm-0.4mm, slight alteration and normal zoning, partial resorption when in contact with orthoclase. Quartz anhedral equant grains, 0.3mm. Orthoclase perthitic, fresh, interstitial or poikilitic up to 5mm. Hornblende subhedral, poikilitic enclosing quartz, plagioclase and opaques, up to 3mm. Biotite

ragged, poikilitic enclosing quartz plagioclase and opaques, approx. 15% chloritic alteration.

8. (K64-207) Granodiorite

Very similar to sample #6. Orthoclase is markedly interstitial, pyroxene is absent and micrographic intergrowths of quartz and orthoclase are common.

Chataway Variety

9. (K64-116a-I) Quartz Diorite

Medium-coarse grained equigranular. Plagioclase exhibits a rough preferred orientation, is euhedral-subhedral, 4mm - 0.5mm, slight alteration, normal zoning. partial resorption where in contact with orthoclase. Quartz is anhedral, interstitial to plagioclase and has strong extinction mosaics. Orthoclase is poikilitic up to 3mm, anhedral and encloses plagioclase, quartz and hornblende. Myrmekite is present at some orthoclase-plagioclase junctions. Hornblende is subhedral up to 2.5mm, fresh and has quartz, plagioclase and opaque inclusions. Biotite is ragged, subhedral, with quartz and opaque inclusions and is approx. 5% chloritised. Sphene is subhedral.

10. (K64-48-I) Granodiorite

Very similar to sample #9 except for slightly coarser grain size. Orthoclase poikilitic up to 5mm. Hornblende strongly poikilitic. Biotite fresh. Myrmekite absent.

11. (K64-144) Granodiorite

Very similar to sample #9. Biotite approx. 2% chloritised.

12. (K64-145) Quartz Diorite

Very similar to sample #9. Myrmekite absent. Biotite approx. 30% chloritised.

LeRoy Variety

14. (K63-209a-I) Granodiorite

Medium-fine grained, equigranular, average grain

size approx. 1.5mm, rough preferred orientation of plagioclase. Plagioclase subhedral-cuhedral, wide range in grain size 5mm - 0.5mm, normal zoning, moderately fresh, partial resorption when in contact with orthoclase, inclusions of opaques and sphene. Quartz may occur as 1) larger (.7mm), poikilitic anhedral grains with plagioclase inclusions and mosaic extinction, or 2) as smaller (.2mm) rounded equant grains which are particularly common as inclusions in orthoclase. Orthoclase is anhedral interstitial and poikilitic enclosing plagioclase, quartz, hornblende and opaques. Hornblende is ragged, subhedral, up to 3mm, poikilitic, enclosing quartz, sphene and opaques. Biotite is ragged, anhedral, up to 1mm, semi-poikilitic enclosing quartz and opaques.

15. (K63-210a-I) Granodiorite

Very similar to sample #14.

16. (K63-185a-I) Granodiorite

Very similar to sample #14.

17. (K64-101) Granodiorite

Very similar to sample #14.

18. (K63-37) Granodiorite

Very similar to sample #14.

GUMP LAKE PHASE

19. (K64-98-I) Granodiorite

Coarse-grained weakly porphyritic. Quartz is coarse grained, anhedral and either interstitial or forming composite? fractured crystals, mosaic extinction and occasional plagioclase inclusions. Plagioclase is cuhedral or subhedral with grain size 5mm to 1mm, slight alteration, weak oscillatory and normal zoning with albitic rims common. Severe resorption of plagioclase when in contact with orthoclase; also some myrmekite present. Orthoclase is perthitic, anhedral, interstitial or coarse poikilitic, enclosing plagioclase and quartz. Biotite is fresh, ragged, anhedral, weakly poikilitic

enclosing plagioclase and quartz, and tends to form clusters associated with accessory opaques.

20. (K64-88) Granodiorite

Very similar to sample #19 except for approx. 10% chloritisation of biotite.

21. (K64-98) Quartz Monzonite

Very similar to sample #19.

BETHLEHEM PHASE

22. (K63-115) Granodiorite

Coarse grained, weakly porphyritic. Plagioclase subhedral, larger crystals exhibit rough preferred orientation, weak oscillatory zoning with variable alteration of zones. Quartz anhedral, interstitial to plagioclase, mosaic extinction common. Hornblende and biotite both ragged, subhedral, poikilitic enclosing plagioclase and quartz. Orthoclase perthitic, anhedral interstitial or poikilitic, slight alteration.

23. (K64-186A) Granodiorite

Very similar to sample #22.

24. (K63-182) Granodiorite

Coarse-grained weakly porphyritic. Quartz may be 1) subhedral, coarse fractured crystals, often composite, or 2) interstitial anhedral grains. Plagioclase is subhedral, 5mm - 0.5mm, exhibits oscillatory/normal zoning and is variably altered. Inclusions of hornblende and quartz are common and partial resorption has occurred when in contact with orthoclase. Orthoclase is perthitic anhedral, interstitial or weakly poikilitic, inclusions of plagioclase, hornblende, sphene and opaques. Some smaller interstitial grains exhibit microcline type grid twinning and this also occurs at edges of some poikilitic grains. Biotite and hornblende ragged, subhedral with slight chloritic alteration at edges.

25. (K63-39) Granodiorite

Very similar to sample #24 except for lack of

microcline type grid twinning in the alkali feldspar and presence of hornblende only as inclusions in salic constituents.

WITCHES BROOK PHASE

26. (K63-171) Granodiorite

Medium-grained, weakly porphyritic. Plagioclase variable grain size 5mm - 0.5mm, poor preferred orientation, euhedral-subhedral, homogenous cores, oscillatory zoned rims, alteration patchy, variable resorption when in contact with orthoclase, inclusions of hornblende and magnetite common. Quartz anhedral, approx. 1mm, equant grains or interstitial, mosaic extinction. Orthoclase perthitic, interstitial or poikilitic, anhedral up to 3.5mm, encloses all other mineral phases. Biotite and hornblende ragged, anhedral 0.5mm, tendency to form clusters with accessory sphene and opaques.

27. (K64-203) Granodiorite

Very similar to sample #26.

28. (K64-102) Granodiorite

Medium to fine grained. Plagioclase subhedral-euhedral, weakly porphyritic, larger crystals (3mm) exhibit rough preferred orientation, normal zoning. Quartz interstitial, weakly poikilitic or anhedral equant grains. Orthoclase interstitial or poikilitic, patchy alteration. Biotite and hornblende fresh, anhedral, fine grained (0.5mm) and ragged, often forming clusters, quartz inclusions common. Sphene interstitial, anhedral-subhedral, associated with mafics.

29. (K63-105-I) Quartz Monzonite

Very similar to sample #28

30. (K63-84) Granodiorite

Very similar to sample #28 except that biotite is approx. 30% chloritised.

31. (K64-17) Quartz Monzonite

Medium grained, equigranular. Plagioclase subhedral

considerable alteration, severe resorption and albitic rims common, traces of oscillatory zoning. Quartz forms anhedral, equant grains with mosaic extinction, also interstitial. Orthoclase perthitic, anhedral-subhedral, considerable alteration, partly interstitial, partly subhedral prismatic, found also as rims of variable width to plagioclase. Biotite fine grained, ragged, anhedral, associated with opaque minerals.

BETHSAIDA PHASE

32. K(63-192A) Granodiorite

Coarse-grained, equigranular or weakly porphyritic. Plagioclase euhedral, average grain size 3mm, composite crystals common, oscillatory zoning, partial resorption when in contact with orthoclase, albitic rims common. Quartz occurs as large, subhedral, fractured grains of variable grain size, 6mm - 2mm. Some graphic intergrowths of orthoclase and quartz. Orthoclase perthitic, coarse, interstitial anhedral or poikilitic subhedral, occasionally partially mantling plagioclase. Hornblende occurs as a single large, poikilitic crystal approx. 1.2 cm, enclosing plagioclase, quartz, magnetite and biotite. Biotite coarse, max. 3mm, ragged, subhedral, inclusions of quartz and plagioclase in outer parts of grains, approx 5% chloritisation. Accessory sphene, opaques, and apatite occur as clusters.

33. (K63-238A) Granodiorite

Very similar to sample #32. Hornblende absent.

34. (K63-231) Granodiorite

Very similar to sample #32, has more porphyritic texture with quartz and plagioclase phenocrysts. Hornblende absent. Biotite fresh, euhedral, coarse grained and weakly porphyritic.

35. (K64-64) Granodiorite

Very similar to sample #32. Hornblende absent.

Appendix 2Modal analyses and calculated chemical compositions

Intrusive Phase		Hybrid			
Sample #	1	2	3	4	
<u>Mode</u>			*	*	
Plagioclase	60.0	55.4	55.0	51.79	
Alkali Feldspar	3.2	5.0	5.0	10.85	
Quartz	17.2	17.7	20.0	20.99	
Biotite	6.0	8.3	8.0	6.18	
Hornblende	0.4	7.3	10.0	-	
Pyroxene	11.2	5.2	1.0	8.80	
Opaque	1.8	0.6	0.77	1.34	
Sphene	0.4	-	Tr	-	
Apatite	-	0.5	Tr	0.06	
Zircon	-	-	Tr	-	
<u>Chemical Estimate</u>					
SiO ₂	60.52	62.28	63.63	64.04	
Al ₂ O ₃	17.12	16.53	16.51	16.11	
Fe ₂ O ₃	3.02	1.67	1.89	2.36	
FeO	3.62	3.74	3.69	3.11	
MgO	2.38	2.66	2.35	2.01	
CaO	7.66	6.16	5.16	5.93	
Na ₂ O	4.04	4.45	4.65	3.98	
K ₂ O	0.93	1.43	1.29	1.94	
H ₂ O	0.14	0.33	0.39	0.14	
P ₂ O ₅	-	0.24	-	0.03	
TiO ₂	0.55	0.46	0.44	0.33	
CaF ₂	-	0.04	-	0.01	

* Modal analysis from Northcote (1969)

Appendix 2 (continued)

Intrusive phase	Highland Valley - Guichon Variety			
Sample #	5	6	7	8
<u>Mode</u>				
Plagioclase	60.3	60.8	52.2	49.9
Alkali Feldspar	1.1	5.0	11.6	9.9
Quartz	12.9	13.9	22.4	27.3
Biotite	11.4	7.1	6.0	3.8
Hornblende	1.8	11.1	6.3	6.2
Pyroxene	7.0	0.6	0.3	0.2
Opaque	4.2	1.5	1.0	1.8
Sphene	1.3	-	0.2	1.1
Apatite	-	-	-	-
Zircon	-	-	-	-
<u>Chemical Estimate</u>				
SiO ₂	56.23	59.94	65.79	67.02
Al ₂ O ₃	16.40	18.16	16.38	14.91
Fe ₂ O ₃	6.05	2.75	1.87	2.79
FeO	5.69	4.01	2.82	2.78
MgO	2.41	2.33	1.55	1.23
CaO	6.06	6.01	4.36	4.34
Na ₂ O	4.60	4.66	4.41	4.29
K ₂ O	1.12	1.34	2.14	1.57
H ₂ O	0.29	0.38	0.26	0.21
P ₂ O ₅	-	-	-	-
TiO ₂	1.15	0.42	0.42	0.80
CaF ₂	-	-	-	-

Appendix 2 (continued)

Intrusive Phase Highland Valley - Chataway Variety

Sample #	9	10	11	12
<u>Mode</u>				
Plagioclase	61.6	55.15	51.8	53.2
Alkali Feldspar	4.8	7.50	14.8	6.8
Quartz	21.4	24.08	21.4	25.2
Biotite	4.2	6.99	6.8	6.8
Hornblende	6.2	4.65	4.8	6.6
Pyroxene	-	-	-	-
Opaque	0.6	0.94	0.4	1.0
Sphene	1.2	0.22	-	0.4
Apatite	-	Tr	-	-
Zircon	-	-	-	-

Chemical Estimate

SiO ₂	65.26	66.13	66.21	66.34
Al ₂ O ₃	17.51	16.67	17.16	15.89
Fe ₂ O ₃	1.25	1.75	1.04	1.89
FeO	2.15	2.73	2.39	2.99
MgO	1.30	1.38	1.38	1.62
CaO	5.60	4.52	4.24	4.46
Na ₂ O	4.87	4.48	4.41	4.40
K ₂ O	0.98	1.64	2.57	1.58
H ₂ O	0.22	0.26	0.26	0.29
P ₂ O ₅	-	-	-	-
TiO ₂	0.87	0.44	0.32	0.55
CaF ₂	-	-	-	-

Appendix 2 (continued)

Intrusive Phase	Highland Valley - LeRoy Variety				
Sample #	14	15	16	17	18
Mode				*	*
Plagioclase	62.8	53.2	50.6	47.	42.23
Alkali Feldspar	8.8	16.4	11.8	16.	20.46
Quartz	15.8	21.4	24.8	26.	28.22
Biotite	4.4	4.2	6.2	6.	3.90
Hornblende	7.2	3.8	5.4	5.	3.21
Pyroxene	-	-	-	-	-
Opaque	0.6	1.0	1.2	0.89	0.63
Sphene	0.4	Tr	-	0.39	0.19
Apatite	-	-	-	-	0.15
Zircon	-	-	-	-	0.02

Chemical Estimate

SiO ₂	62.57	65.40	66.48	68.11	70.48
Al ₂ O ₃	19.22	18.11	16.16	15.32	14.99
Fe ₂ O ₃	1.30	1.60	2.08	1.64	1.17
FeO	2.34	1.96	2.81	2.51	1.71
MgO	1.46	0.93	1.39	1.31	0.87
CaO	6.16	4.88	4.20	3.47	3.12
Na ₂ O	4.67	4.33	4.25	4.31	4.15
K ₂ O	1.56	2.41	2.07	2.60	2.96
H ₂ O	0.24	0.17	0.25	0.24	0.16
P ₂ O ₅	-	-	-	-	0.08
TiO ₂	0.47	0.20	0.31	0.49	0.30
CaF ₂	-	-	-	-	0.01

Appendix 2 (continued)

Intrusive Phase		Gump Lake		
Sample #		19	20	21
<u>Mode</u>	*			
Plagioclase		37.25	30.6	36.6
Alkali Feldspar		16.77	22.4	23.4
Quartz		39.16	39.8	38.2
Biotite		5.24	4.8	1.6
Hornblende		0.75	-	-
Pyroxene		-	-	-
Opaque		0.66	0.6	0.2
Sphene		-	-	-
Apatite		0.09	-	-
Zircon		0.09	-	-
<u>Chemical Estimate</u>				
SiO ₂		74.50	76.04	76.35
Al ₂ O ₃		13.09	12.22	13.56
Fe ₂ O ₃		1.14	1.06	0.34
FeO		1.63	1.47	0.47
MgO		0.66	0.53	0.17
CaO		2.47	1.86	2.25
Na ₂ O		3.59	2.83	3.73
K ₂ O		2.50	3.66	3.02
H ₂ O		0.14	0.12	0.04
P ₂ O ₅		0.04	-	-
TiO ₂		0.21	0.19	0.06
CaF ₂		0.01	-	-

Appendix 2 (continued)

Intrusive Phase		Bethlehem			
Sample #	22	23	24	25	
Mode	*	*			
Plagioclase	59.48	55.45	53.3	50.8	
Alkali Feldspar	13.38	8.35	15.0	12.4	
Quartz	18.59	25.87	26.2	33.4	
Biotite	1.76	4.85	3.2	2.8	
Hornblende	4.95	4.48	1.3	0.6	
Pyroxene	-	-	-	-	
Opaque	1.06	1.26	0.5	-	
Sphene	0.52	-	0.4	-	
Apatite	0.12	Tr	-	-	
Zircon	0.06	Tr	-	-	

Chemical Estimate

SiO ₂	65.35	67.91	69.97	73.37
Al ₂ O ₃	17.92	15.88	16.46	15.51
Fe ₂ O ₃	1.71	2.07	0.87	0.15
FeO	1.74	2.43	1.19	0.70
MgO	0.88	1.13	0.52	0.38
CaO	4.93	3.77	3.63	3.46
Na ₂ O	5.03	4.85	4.90	4.39
K ₂ O	1.82	1.53	2.01	1.84
H ₂ O	0.14	0.20	0.10	0.08
P ₂ O ₅	0.06	-	-	-
TiO ₂	0.41	0.24	0.35	0.12
CaF ₂	0.01	-	-	-

Appendix 2 (continued)

Intrusive Phase

Witches Brook Phase

Sample #	26	27	28	29	30	31
Mode	*	*	*	*	*	*
Plagioclase	53.37	51.33	45.0	40.40	41.0	30.15
Alkali Feldspar	11.07	12.66	17.0	21.09	20.0	26.23
Quartz	26.36	28.06	28.0	28.38	28.0	41.38
Biotite	4.87	5.54	5.0	3.11	5.0	1.84
Hornblende	3.22	1.87	3.0	4.50	5.0	-
Pyroxene	Tr	-	-	-	Tr	-
Opaque	1.06	0.34	0.96	0.73	0.3	0.39
Sphene	0.26	0.14	0.60	1.75	0.3	-
Apatite	Tr	-	-	Tr	-	-
Zircon	Tr	Tr	-	-	-	-

Chemical Estimate

SiO ₂	67.54	70.41	69.62	69.80	70.18	77.73
Al ₂ O ₃	16.52	15.80	14.91	14.42	14.75	12.17
Fe ₂ O ₃	1.75	0.78	1.63	1.31	0.86	0.55
FeO	2.13	1.67	2.09	1.77	2.03	0.58
MgO	0.95	0.85	0.95	0.96	1.28	0.18
CaO	4.40	3.29	3.15	3.62	3.21	0.65
Na ₂ O	4.27	4.88	4.33	4.03	4.09	3.96
K ₂ O	1.88	1.84	2.59	2.82	2.95	4.07
H ₂ O	0.17	0.17	0.18	0.16	0.22	0.04
P ₂ O ₅	-	-	-	-	-	-
TiO ₂	0.36	0.31	0.55	1.10	0.42	0.06
CaF ₂	-	-	-	-	-	-

Appendix 2 (continued)

Intrusive Phase		Bothsaida Phase			
Sample #	32	33	34	35	
<u>Mode</u>		*			
Plagioclase	58.92	57.97	53.	46.21	
Alkali Feldspar	10.82	14.55	11.	5.88	
Quartz	19.70	22.08	30.	35.22	
Biotite	0.51	3.62	4.	11.88	
Hornblende	7.05	0.14	0.23	0.42	
Pyroxene	-	-	-	-	
Opaque	2.94	1.24	0.66	0.44	
Sphene	-	0.23	0.26	-	
Apatite	0.02	0.18	0.26	0.02	
Zircon	-	-	Tr	-	

Chemical Estimate

SiO ₂	64.25	67.79	70.90	72.34
Al ₂ O ₃	16.59	17.13	15.74	13.84
Fe ₂ O ₃	4.16	1.82	1.07	0.79
FeO	2.85	1.54	1.30	2.54
MgO	1.02	0.40	0.45	1.20
CaO	4.34	3.52	3.59	2.43
Na ₂ O	5.09	5.35	4.67	4.28
K ₂ O	1.42	2.00	1.74	1.88
H ₂ O	0.15	0.09	0.10	0.27
P ₂ O ₅	0.01	0.09	0.13	0.01
TiO ₂	0.12	0.26	0.29	0.42
CaF ₂	Tr	0.02	0.02	Tr

Appendix 3 Biotite Electron Microprobe Analysis

1) Sample Selection and Preparation

Biotite samples were prepared as grain mounts rather than as thin sections of rocks since this allowed a much more representative sample to be examined. Approximately half of the samples used were originally concentrated by K.E. Northcote for use in K/Ar age dating studies of the batholith. The remaining samples were separated from a crushed hand size rock sample by combined sieving and hand picking techniques. Several grains from each sample were cold mounted in epoxy resin cylindrical mounts and polished. For electron microprobe analysis a perfectly flat sample surface is required in order to minimise irregular absorption effects on the X-rays generated within the sample. A perfectly flat sample surface is extremely difficult to attain with biotite samples because of the extremely fine scale nature of the perfect basal cleavage present in micas. Initial hand polishing on a glass plate with 950 carborundum grit was employed to expose the biotite grains at the surface of the epoxy mount. Secondary polishing was done with tin oxide powder on a rotary polishing machine with cloth laps. This second stage often produced sample surfaces which were deemed to be sufficiently well polished. If further polishing was necessary this was achieved using 1μ

and $\frac{1}{4}$ μ diamond paste on a silk lap rotary polishing machine. All mounts were carbon-coated with a coat thickness corresponding to a purple-blue colour on polished brass. (Smith, 1965)

2) Standards

In order to minimise differential absorption and fluorescence effects between samples and standards it was decided that a number of chemically analysed natural biotites would be used as standards. The author is particularly grateful to Dr. J.H.Y. Rimsaite of The Geological Survey of Canada for her help in providing the standards prefixed R in Table XI. Chemical analyses and physical properties for these standards have been published by Dr. Rimsaite in G.S.C. Bulletin #149 (1967). The author would also like to thank Dr. J.A. Gower of the Geology Department, University of British Columbia for providing the standards prefixed B in Table XI. Partial chemical analyses for the B standards were carried out by 'rapid' methods by the Geological Research Department of Cominco Ltd. at Trail, B.C.

3) Instrumentation and Technique

The instrument used was a Japanese Electron Optics Laboratories JxA-3A(3140) which has a normally incident electron beam, a spectrometer take-off angle of 20° , and is equipped with gas flow proportional counters. All

analyses were carried out at an electron excitation potential of 25kv. and sample currents approximately .08 μ A, using a spot size of approximately 5 μ . The electron beam current was monitored between each analysis by returning to a Cadmium standard and checking that the sample current on this standard was steady. Slight fluctuations of the Cadmium standard current were adjusted by means of the condenser lens bias control.

Simultaneous analyses were made for $\text{MgK}\alpha$ and $\text{FeK}\alpha$, using a mica crystal for $\text{MgK}\alpha$, and a quartz crystal for $\text{FeK}\alpha$, in the two spectrometers. Counting response for $\text{FeK}\alpha$, was good, averaging 1,500 counts/sec. for a sample containing 15 Wt% Fe. Counting response for $\text{MgK}\alpha$, however, was extremely poor, average 30 counts/sec for a sample containing 8 Wt% Mg. Peak to background ratios for an average sample were approximately 200:1 for $\text{FeK}\alpha$, and 8:1 for $\text{MgK}\alpha$. Background counts were found to be the same at $1^\circ 2\theta$ above and $1^\circ 2\theta$ below the peak position, and thus background counts were taken for all analyses at $1^\circ 2\theta$ below the peak position.

In view of the low counting rates for $\text{MgK}\alpha$, it was necessary to count for relatively long periods of time at any single spot. Repeated ten second analyses of the same spot showed that after approximately 50 secs there was a notable decrease in the counting rates for both

MgK α and FeK α , presumably due to surface contamination build up. Thus analyses of a single spot were carried out for 40 sec time intervals.

In order to check for sample inhomogeneity 3-5 spots were analysed per grain and 5 grains analysed per sample. In addition several of the samples were checked for compositional zoning by making linear traverses from grain cores to grain boundaries. No compositional zoning was observed in any of the standards nor in any of the samples investigated.

Fig. 17 is a plot of composition against total counts collected per 40 secs during a single running period for the standards used in the present study. The standards lie on a very slightly curved line which has a tendency to increase slope at higher counting rates. The Guichon biotite samples all lie within the range of standards R.24 - R.11 and in this range the correlation curve of total counts collected to composition is effectively a straight line.

The relative errors in analysis may be gauged by inspection of Fig.17. Relative errors in the estimate of compositions for the Guichon batholith samples are estimated at ± 0.35 Wt% Mg and ± 0.25 Wt% Fe. This estimate takes into account the 'fitting' of correlation

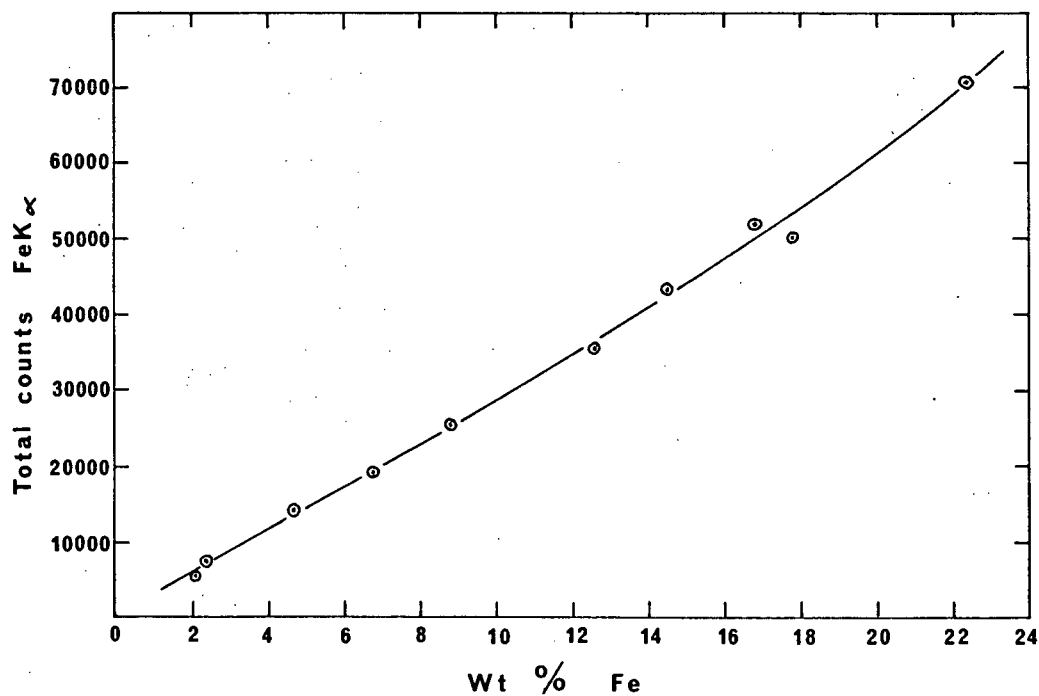
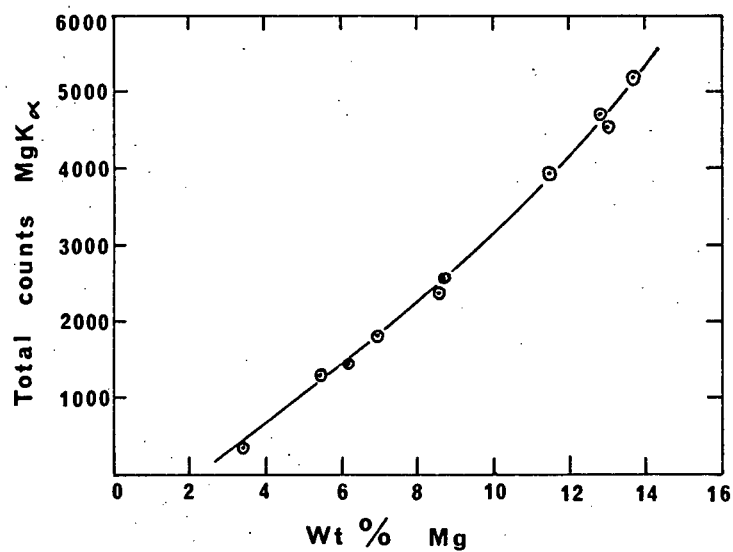


Fig. 17 Microprobe analyses. Total counts observed as a function of composition for biotite standards. Circles approximate one standard deviation of total counts observed.

Table XI Data used in construction of Fig 17

Standard #	Wt% Mg chemical	Average Total counts MgK α (40 secs)	σ counts	$\bar{E}\%$ counts	σ Mg%
R.31	3.49	352	18	5.15	.1
R.24	5.53	1300	80	6.1	.2
R.26	6.21	1468	70	4.7	.15
B.12	6.99	1834	50	2.7	.125
R.11	8.63	2380	160	6.7	.4
R.13	8.80	2488	112	4.5	.25
B.16	11.46	3944	174	4.4	.25
B. 8	12.84	4712	124	2.6	.15
R. 7	13.15	4514	148	3.3	.20
B.18	13.69	5228	46	0.8	.1

Standard #	Wt% Fe chemical	Average Total counts FeK α (40 secs)	σ counts	$\bar{E}\%$ counts	σ Fe%
B.18	2.1	5420	164	3.0	.1
B. 8	2.4	7612	164	2.1	.1
R. 7	4.71	14368	184	1.3	.1
B.16	6.8	19408	440	2.3	.2
B.12	8.83	25432	344	1.4	.2
R.11	12.57	35576	1200	3.4	.4
R.13	14.49	43588	564	1.3	.25
R.26	16.81	52192	2432	4.6	.6
R.24	17.88	50248	1348	2.7	.4
R.31	22.42	70560	956	1.4	.25

σ counts 1 standard deviation from the average value
obtained from several spot analyses on
several grains from each sample

σ Mg% and σ Fe% have been estimated from a knowledge of
 σ counts and the correlation curves of
Fig. 14

curves, sample inhomogeneity and the statistical variation of X-ray generation. Total instrumental drift was checked by analyses of standards before, during and after each set of unknown samples. Drift was found to be less than one standard deviation in the accumulated counts for all of the standards employed.